5-2008

A Systems Approach to the Design of a Two Dimensional Cell Printer

Albert Hill
Clemson University, ahill@clemson.edu

A SYSTEMS APPROACH TO THE DESIGN OF A TWO DIMENSIONAL CELL PRINTER

A Thesis
Presented to
the Graduate School of
Clemson University

In Partial Fulfillment
of the Requirements for the Degree
Master of Science
Electrical Engineering

---

by
Albert Martin Hill
May 2008

Accepted by:
Timothy Burg, Committee Chair
Richard Groff, Co-Committee Chair
Karen Burg
Thomas Boland
Darren Dawson

ABSTRACT

Tissue engineering research has the potential to improve the current opportunities for replacement organs and tissues. Precise placement of cells has proven difficult in the early stages of this research. Bioprinting is an important research area that has the potential to accurately position cells and biological materials for tissue engineering. This paper describes the attempt to obtain micrometer accuracy in the placement of cells using a systems approach and technology derived from the Hewlett Packard 500 series of printers and their cartridges the HP26 series. The paper discusses the research and design of a custom printing system that allows control over printing parameters used to fire a droplet from the inkjet cartridge that include resolution, firing duration, and print speed. The proposed system also allows a larger workspace to print and the ability to print multiple cell types. These abilities are necessary in order to further research into this method of tissue engineering.

DEDICATION

I would like to dedicate my work to my parents and grandparents. Without the love and support they have provided me through my studies, I would not have had the opportunities that have shaped my life. They have been the emotional and physical support to encourage me when I have felt lost and discouraged. I could not have asked for a more loving and caring set of parents or grandparents to guide and teach me through life's lessons. Therefore I dedicate this small portion of the work, that hopefully will provide a tool to eventually one day improve the lives of others, in honor of them for the countless gifts of themselves in the bettering of myself.

ACKNOWLEDGMENTS

I would like to thank the National Science Foundation for supplying our research with the Emerging Frontiers in Research and Innovation Grant and also thank the United States Department of Defense for their sponsoring of our research with the Era of Hope Scholar Award. Also I would like to thank Cheryl Parzel and Matthew Pepper for their continued support and work towards the Bioprinting project at Clemson University. Without their support and efforts this work would have been impossible.

TABLE OF CONTENTS

Page

Table of Contents (Continued)

LIST OF TABLES

Table Page

LIST OF FIGURES

List of Figures (Continued)

Figure Page

List of Figures (Continued)

Figure Page

List of Figures (Continued)

Figure Page

List of Figures (Continued)

Figure Page

CHAPTER ONE
INTRODUCTION

Bioprinting is a relatively new area of research in the field of Tissue Engineering. Investigators have shown that patterns of proteins and cells can be printed using standard inkjet printers as a delivery system. This work has largely been done using the proprietary drivers and embedded software of the Hewlett-Packard (Hewlett-Packard, Palo Alto, CA) [2,3,10,16,17,18] and Canon (Canon, Tokyo, Japan) inkjet printers [13,11]. This approach has provided a valuable proof of concept. However, this printing process is optimized for printing ink and cannot directly be manipulated by the user. This research will examine current bioprinting techniques and propose a system that will allow more extensive control over the delivery of biological material using an adapted Hewlett-Packard cartridge with an integrated printhead.

What is Tissue Engineering?

Tissue engineering has been defined as the field of study that, "targets the use of engineering and life sciences to develop biological substitutes that restore, maintain, or improve tissue function" [14]. In broader terms, the goal of tissue engineering as a medical therapy is to replace tissue damaged through trauma or disease processes with the original tissue. In tissue engineering, cells from the patient are collected and processed to create the new engineered tissue. Creating an autologous implant, made using the existing tissue material to provide seed cells, limits the effects of rejection when the tissue is replaced [8].

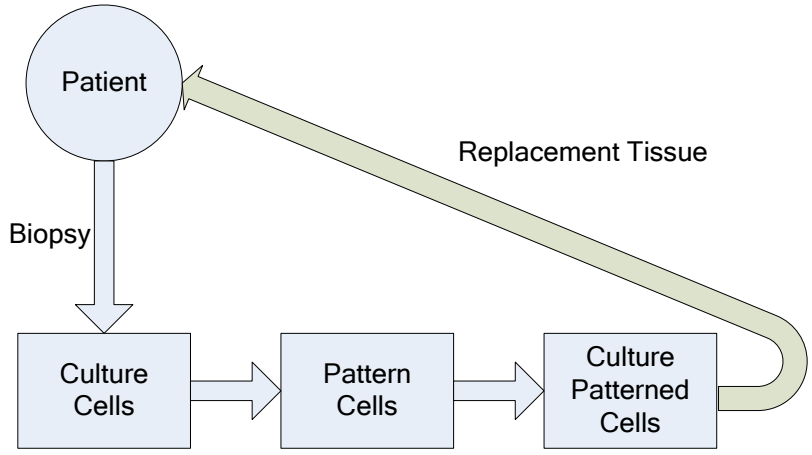

Figure 1-1 Tissue Engineering Process

The tissue engineering process is depicted in Figure 1-1. The cells are first harvested from the patient and then multiplied in culture. These cells are then deposited on a tissue scaffold, or supporting structure of biomaterial, to allow the cells to proliferate and adhere to a surface defining the eventual shape of the tissue [8]. The scaffold may be a single material, such as foam, or may be a composite such as smaller beads suspended in a gel [3]. The new tissue structure is then implanted in the patient. The scaffold is typically an absorbable material that will solubilize as the cells grow until only the cellular component remains.

Many approaches to tissue engineering seek to "randomly" apply a mixture of cell types to the scaffold. Although this approach has yielded many results, it has been suggested that tissue engineering should seek to recreate well defined tissue or organ structures [17]. This approach would require the ability to place cells accurately in a pattern that will then grow in a predictable manner. An illustration of patterning cells to build a human mammary gland, tissue is shown in Figure 1-2. On the left is the original tissue (sec. 31-4636 Carolina Medical Supply) and on the right is an approximation of the

tissue that might be obtained with cell patterning. In Figure 1-2 the orange circles represent the interlobular connective tissue of the patterned gland and the purple circles represent the secretory tubules in the pattern to reproduce a viable tissue sample. Without precise placement of cellular material, complicated tissue patterns cannot be replicated or seeded onto cellular scaffolds. A more precise cellular deposition system is needed to fully exploit this approach.

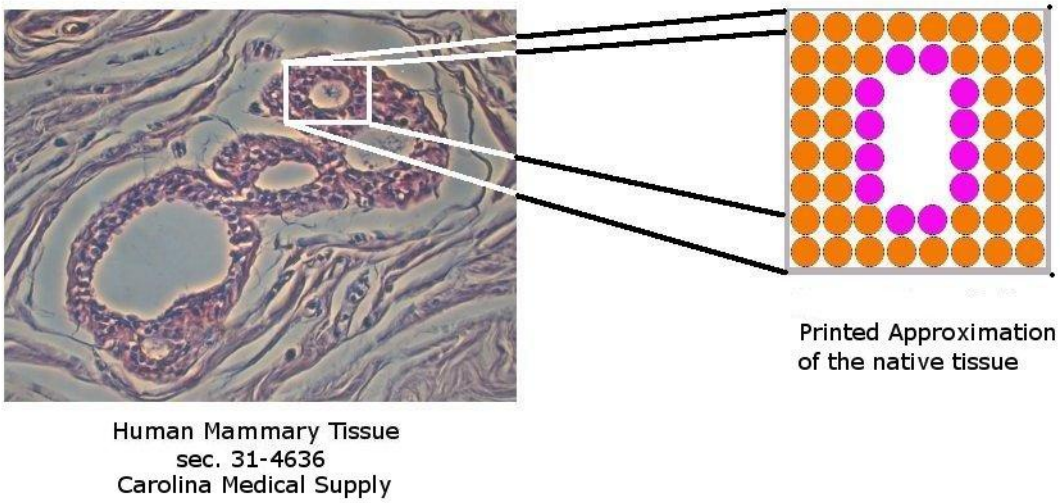

Figure 1-2 Example of Human Mammary Gland and a Printed Approximation

Precision Cell Placement

Bioprinting has been defined as "the application of the principles of rapid prototyping technology (i.e. layer by layer deposition of cells or matrix)" to the problem of tissue engineering [10]. Multiple approaches to arranging cells have been proposed including: 1. Drop-on-demand printers, 2. Continuous stream printers, and 3. Laser tweezers. Currently this process is done through use of several different drop-on-demand methods: using a commercial printer with modified cartridges and printheads [18];

adapting a printer with a needle and pump printhead [16]; or using a pipette to place cellular material. A comparison of the three systems is presented in Figure 1-3 where the operation of each system is illustrated.

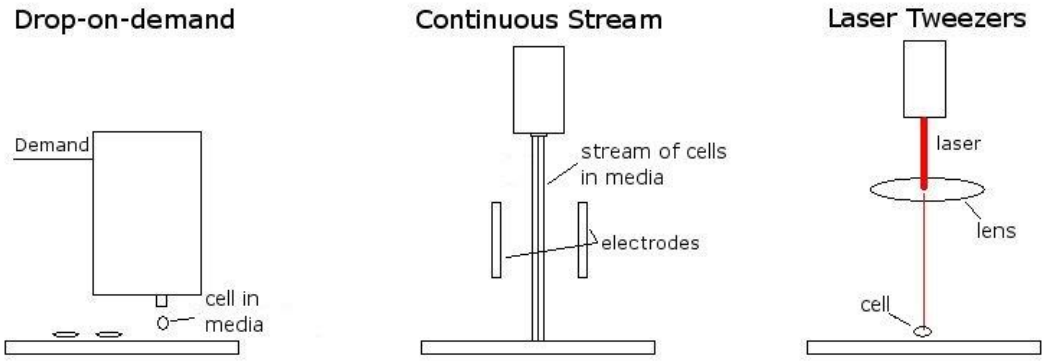

Figure 1-3 Different Patterning Systems

The use of a laser beam through a microscope objective to move dielectric particles is what has been defined as laser tweezers. The process works on the principle that the electric field gradient of a focused laser beam can exert forces on micron sized particles in a liquid which allows them to be moved and positioned into patterns [1]. This process can then be used in a manner similar to tweezers to drag and arrange particles into a pattern. This process is not very well suited for bioprinting applications due to the time it would take to construct a very large pattern in this manner. Therefore this method has not been actively pursued as a solution to precision placement in tissue engineering.

Continuous stream printers eject a constant stream of ink and only the direction of the ink is controlled via electromagnetic field [11]. The ink is adjusted via a time varying signal applied to electrodes outside the printhead and therefore is adjusted to the corresponding location of the input pattern. The stream must be directed into a waste

collection point when no ink deposition is needed. This type of printer allows for very fine streams of ink to be ejected however it has many limitations when attempting to use it with bioprinting. These limitations include complex control parameters associated with generating electromagnetic fields to guide the ink and the inability to have discrete high resolution patterns since the ink is continuously flowing. These limitations keep the use of continuous stream printers from being used in the design of bioprinting systems.

Drop-on-demand printers are defined as printers that can eject discrete amounts of ink at high resolution with small volume drops only after a demand signal is received [11]. The discrete patterns produced are a result of the print cartridge with printhead and the positioning system, the resolution of these printers continues to evolve as technology for the number of nozzles, their spacing, and their diameter evolves. These types of printers will allow for micron level accuracy in positioning cells which is important in the creation of viable tissue [11]. Review of the literature suggests that the drop-on-demand systems appear to be the system most well suited for bioprinting applications. Drop-on-demand inkjet printers will impact the tissue engineering community by "commercialization and cost cutting" [15]. This is due to its cost, accuracy, and speed. Commercial ink jet printers have been proposed as early as 2003 [16] as a solution to the cell placement challenge in tissue engineering.

Inkjet systems are a form of the drop-on-demand printers, and typically utilize piezoelectric or thermal mechanisms to eject the media from the print cartridge's printhead. Inkjet printers fall into the drop-on-demand category of printers since the system places a discrete matrix of dots on the print media to form patterns that

correspond to the input to the system, e.g. an image to be printed. Therefore choosing a cartridge and printhead for the specific material based upon the size of the particulate in the "bio-ink" and the desired print resolution are important considerations when adapting drop-on-demand printers for bioprinting.

Piezoelectric printers operate on the principle of a piezo device inside the firing chamber expanding when a voltage is applied and the resulting change in volume in the nozzle chamber ejects an ink drop. Various waveforms and frequencies can be used to drive the piezo device but have varying effects due to the acoustic resonance of the printhead [13]. The process is depicted in Figure 1-4.

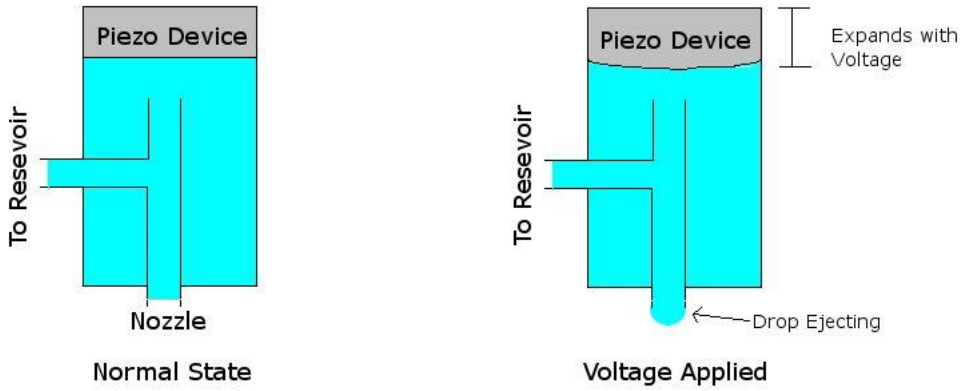

Figure 1-4 Piezo Printer Operation

Thermal inkjet printers operate on a process in which heating a thin-film resistor inside the print chamber forms a bubble and the pressure from the bubble creation forces an ink drop to be ejected. As the drop is ejected, the bubble rapidly cools and shrinks and liquid from above the firing element fills the void left by the evacuated drop. This process is illustrated in Figure 1-5.

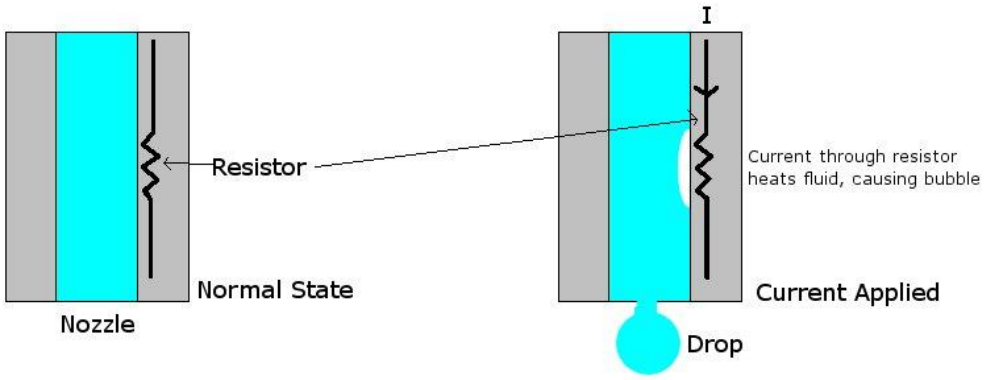

Figure 1-5 Thermal Printer Operation

The piezo printers use high frequency vibrations in the print media that push the drops out of the nozzle while the thermal printers create bubbles that expand in the firing chamber and displace the ink to force a drop to eject. Thermal printers create high temperature increases around the heating element, whereas piezo printers create mechanical vibrations in the liquid in the firing chamber. Piezo printers have been shown to successfully print and sustain viability in mammalian cells [13] whereas the same has been shown in thermal inkjet printers [18].

The cost of inkjet technology has steadily decreased since its inception in the 1980's. Print cartridges and printheads can be reused multiple times with the removal of the ink and the actual printers can be obtained for less than fifty US dollars. These abilities along with the ink-jets ability to place drops at resolutions of 300 dots per inch make ink-jet technology a forerunner in the development of Bioprinting techniques.

Thermal Inkjet Printing as a Bioprinting Solution

Thermal inkjet printing of cells can be traced to the patent of Thomas Boland submitted in 2003 [US Patent # 7,051,654]. Currently, most inkjet printing of living cells

uses the printer as a black box where the method of printing is completely hidden from the user. Current methods include using a modified HP 550 DeskJet printer and a word processing application to pattern the output of the printer [2]. This method provides little insight into the actual effects of set parameters determined by Hewlett-Packard through their hardware and software design of the printer.

The current method has been shown to provide biological results where cells that are printed via the thermal ink jet process have been shown to retain 90% viability, or that the cells remain metabolically active [17]. Therefore the process has the potential to print patterns of cells and have them survive the process and proliferate. This is due to the fact that the thermal process used to print the cells only raised the temperature of the surrounding liquid by four degrees Celsius [17].

The Bioprinting literature also lists the different solutions that have been used in the HP26 series cartridges as “bio-ink” [18]. Table 1-1 lists the substances that are known to print from the cartridge and printhead.

Bio-ink	
Water	Serum-free cell media
Ethanol	Collagen
Calcium chloride	Laminin
Algenate	Fibrin

Table 1-1 Printable Bio-inks

Calcium chloride and alginate are used for structuring scaffolds that provide support and nourishment for the eventual printed cells [2]. The “bio-ink” most commonly used to print cells is the serum-free cell media, which is simply a solution of salts and glucose that provide nourishment for the cells. With the current modified HP 500 series printer there is no direct method to change printing parameters that may affect performance of printing the different “bio-inks”.

However with the current process the actual placement of cells is not fully user determined, they are placed according to the proprietary firmware of the printer, the driver in the operating system, and the software package, e.g. Adobe Illustrator. The print resolution is limited by the resolution of the printer, not necessarily the cartridge, and cannot be changed by the user. Also using the current method there is no method to determine the statistical probability of obtaining a cell when a drop is ejected from the nozzle. Current research into using thermal inkjet printers has also been limited to the

height of the printhead and the width of the travel of the HP 500 series printer (50 dots high by 8.5 inches wide) used to print the pattern [2]. This limitation is due the fact that the printhead only has one degree of freedom in its movement while the platform for the print media remains stationary; that is, the mechanism that feeds paper to produce 2D paper printing cannot be easily adapted to media such as glass slides. This is definitely a limitation to the advancement of the technology, since it provides a pattern size constraint on the system.

The preceding limitations of the current generation of bioprinting tools has led to the need for a customizable tool that allows the end user to study the different printing parameters associated with cellular solutions [4]. These include, but are not limited to, the amount of energy delivered to a droplet of "bio-ink", proximity of printed dots, and the statistical likelihood of printing a cell in a drop. With these parameters as a driving force, a custom printing system was proposed that would allow the end user to have the ability to study the effects of these parameters on various "bio-inks" and cells and retain the same metabolic stability of the cells post printing.

With these driving factors we propose building a custom system to be used in bioprinting. The custom system will be built around knowledge gained from reverse engineering the printing system of an HP 500 series printer, and involve integrating custom hardware and software with commercial positioning systems. This system will provide the flexibility for new research to be achieved in the field of bioprinting.

Using the HP26 Cartridge for Bioprinting

The HP 26 cartridge was designed by Hewlett-Packard to operate in their 500 series line of thermal inkjet printers and is integrated with a printhead. The cartridge operates with a thin-film resistor inside the print nozzle, that when current is passed through the resistor, the surrounding liquid heats causing a bubble to form and eject a drop from the nozzle. This process is illustrated in Figure 1-5. To develop the cartridge some technical problems had to be solved, e.g. developing an improved thin film design for the heating elements to extend the life of a printhead that would be fired at a higher frequency than its predecessor, and switching from a glass substrate to a silicon substrate to improve thermal conductivity. Also a thin coating of polymer must also be placed over the silicon substrate to separate the nozzle resistors and provide insulation. The printhead was not the sole problem in designing the cartridge, the firing chamber had to be designed to eject a consistent ink drop and an interconnect system for the nozzles had to be developed [5]. All of the design features that HP solved led to the conclusion that to construct a custom system, the operation of the HP26 cartridge must be understood and used as the focus of the design.

The main component of a printing system is its printhead, which in the HP500 series is integrated into the HP26 cartridge. The rest of the printing system is concerned with the positioning the printhead and moving the print media. This leads to the conclusion that the only component necessary in constructing a bioprinter is the print cartridge itself. The cartridge is used to deliver the “ink” solution inside the cartridge when the cartridge is instructed. This is done in a fashion where drops can be delivered

whenever they are demanded from the system. The positioning system manipulates and commands the cartridge to fire at precise locations that will accurately deposit drops wherever the input pattern specifies. These commands are easily reconstructed and motion systems are commercially available that provide more precise control over position. This confirms that development of a custom bioprinter centers around the control and understanding of the operation of the print cartridge.

Commercially available systems for bioprinting ImTech (ImTech, Corvallis, OR) and MicroFab (MicroFab, Plano, TX) are similarly designed and built around the print cartridge and printhead. ImTech builds custom printing systems for multiple applications. The IJet S and E models can print a 50 nozzle HP inkjet cartridge. They operate by moving the printhead as do the original printer systems and can print with two cartridges at a time. The ImTech systems can fire up to 12,000 drops per second and accept input as a monochrome bitmap image. The x-y positioning accuracy of the system is 25 microns with a repeatability of 15 microns. The maximum velocity for the IJet models is 1016 mm/s. The systems can begin printing anywhere in the workspace that is part of their system defined dispensing zone. MicroFab creates custom systems as well; however, they operate with a fixed printhead that only moves in the z-direction. The print media in their Jetlab series of printers moves to provide the patterning of the printed media. Their system has an x-y accuracy of 30 microns and a repeatability of 20 microns. The maximum velocity of the Jetlab series is 50 mm/s and the maximum acceleration of the system is 1500 mm/s^2. The Jetlab model is designed around a custom piezoelectric

printhead that can be heated or operated at room temperature and has the option of mounting a vision system.

These commercial systems provide control over the printing and multiple features not available in modified inkjet printers. They however are costly and a custom system can be designed and integrated that provide more features and potential for expansion, including additional cartridges. Therefore the commercial solutions have been rejected as alternatives to the modified inkjet printers and a custom designed system has been proposed.

Organization of Thesis

The goals of the Bioprinting project were to design and build a system that could accurately place cells while allowing the end user access to the low-level parameters that affect printing from an HP26 cartridge. This thesis describes the evolution of such a design from the advanced understanding of an HP printer through the construction of a prototype 2D printer.

Chapter 2 initiates a design plan that begins with understanding a HP 520c printer. Detailed physical and literature analysis produced an understanding of the thermal inkjet process.

Chapter 3 builds on this knowledge by developing a design of a custom electronic interface to the cartridge that was tested in simulation and with a prototype. The project was to implement standard control hardware and use custom electronics to control the firing of the cartridge. These sytems allow for simple studies that were not accessible with the previous bioprinting technologies such as studying the probability of printing a

cell at different concentrations of cells in the “bio-ink” and studying the effect of single drop patterns as they grow in culture.

Chapter 4 describes the integration of the final version of the prototype into a real-time software solution and positioning system that integrated every component into a functioning Bioprinter. When the integrated system was completed, testing of the functionality and accuracy of the overall system was performed to understand the results in the contexts of our original goals set out for the project.

CHAPTER TWO
REVERSE ENGINEERING THE HP26 CARTRIDGE USING A HP 520C PRINTER

The HP26 cartridge was identified as a potential solution to printing cells and has already been demonstrated in the HP 500 series printers [16]. In order to exploit the technology in the HP26 cartridge, the cartridge was studied in the operational context of the HP 520C printer and an operational model was developed. This chapter presents an interface description of the HP26 cartridge that can be used to control the cartridge independent of the printer. This interface description was developed measuring signals generated by the HP 520C printer to control the HP26 cartridge by examining the electronics inside the printer, and reviewing relative articles in the Hewlett-Packard (Hewlett-Packard, Palo Alto, CA) design journals.

Introduction to the HP26 Printer Cartridge

The HP26 Cartridge is an ink cartridge designed to operate in the HP 500 series of printers. The cartridge has a chamber to hold the ink, a printhead that contains the nozzles, and a flex circuit with 56 connections to access the cartridge. The print cartridge can be seen in Figure 2-1 from several different views, the rear view shows the flex circuit connection points and the bottom view shows the printhead.

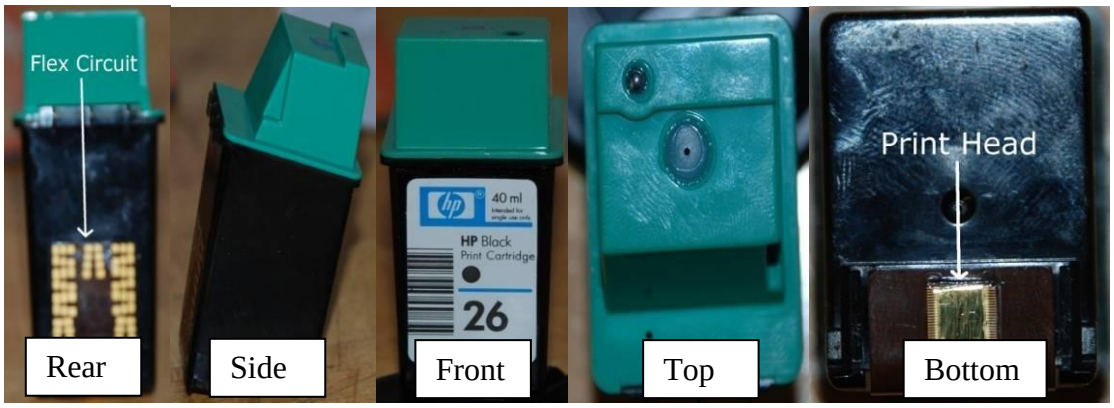

Figure 2-1 Multiple Views of HP26 Cartridge

A magnified view of the printhead is shown in Figure 2-2 where the location, size, and relative distance of the nozzles are seen. The cartridge was designed to print black ink through fifty (50) nozzles.

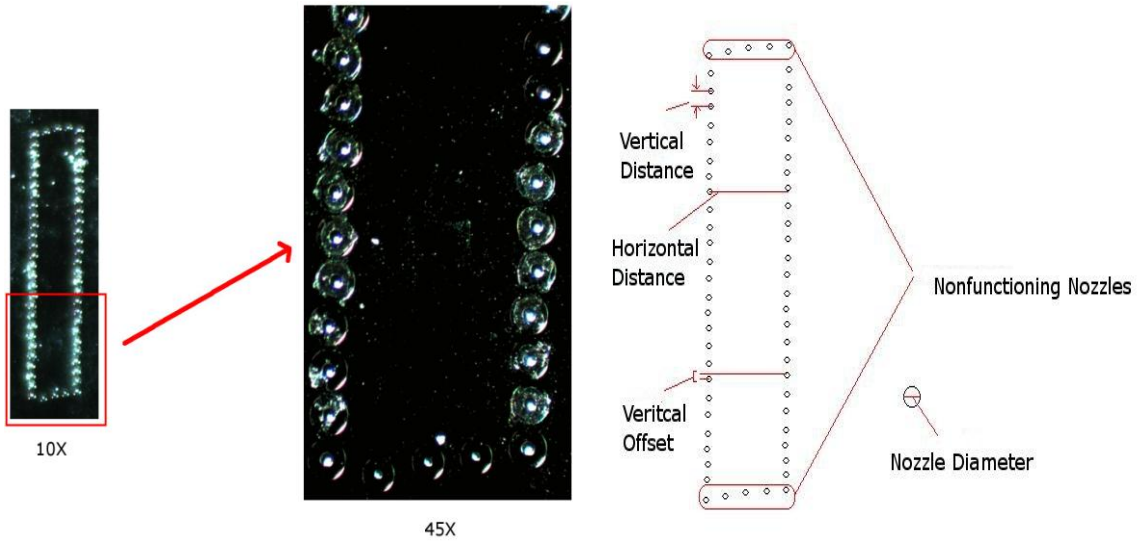

Figure 2-2 Printhead at 10x, 45x, and Diagram of Measurements

The dimensions of the nozzle constellation were measured using a Zeiss 2000-C stereoscope (Carl Zeiss Inc, Oberkochen, Germany) with a PixeLINK PL-A622 firewire camera (PixeLINK, Dayton, OH) to capture the images. The captured image of the printhead was imported into ImageJ (http://rsb.info.nih.gov/ij/) along with a reference

image that contains an object with a one millimeter feature taken at the same magnification, used to calibrate the camera. Measurements of the features shown in Figure 2-2 are summarized in Table 2-1.

Dimension	**Measurement**	**From Literature [9]**
Vertical Distance Between Nozzles in Column	177 microns	169 microns
Horizontal Distance Between Opposing Nozzles	863 microns	847 microns
Diameter of Individual Nozzle	48 microns	50 microns
Vertical Offset Between Corresponding Nozzles in Opposing Columns	45 microns	N/A

Table 2-1 Measured Dimension of HP26 Cartridge

These results compare favorably to the data provided in the literature where the nozzles are separated 169 microns apart vertically with the two columns of 25 nozzles separated horizontally by 847 microns [9]. The difference between these measurements could be a result of difficulty in identifying repeatable measurements points on the nozzles and the accuracy of the reference image.

The internal components of the HP26 cartridge were discovered when the cartridge was disassembled and the ink removed. Figure 2-3 shows the cartridge after the top was removed using the cutting wheel of a Dremel tool (Dremel Inc, Racine, WI). The cartridge has a mesh filter that keeps solid material i.e. particulate that may be in the ink, from entering the nozzle chamber. There is also an air bladder and spring inside the cartridge. We hypothesize that the purpose of the bladder may be to provide back pressure inside the cartridge to stop ink from flowing out of the cartridge; however, this has not been verified. These components and a cutaway view inside the cartridge can be

seen in Figure 2-3 where the filter is seen still inside the cartridge and the air bladder has been removed.

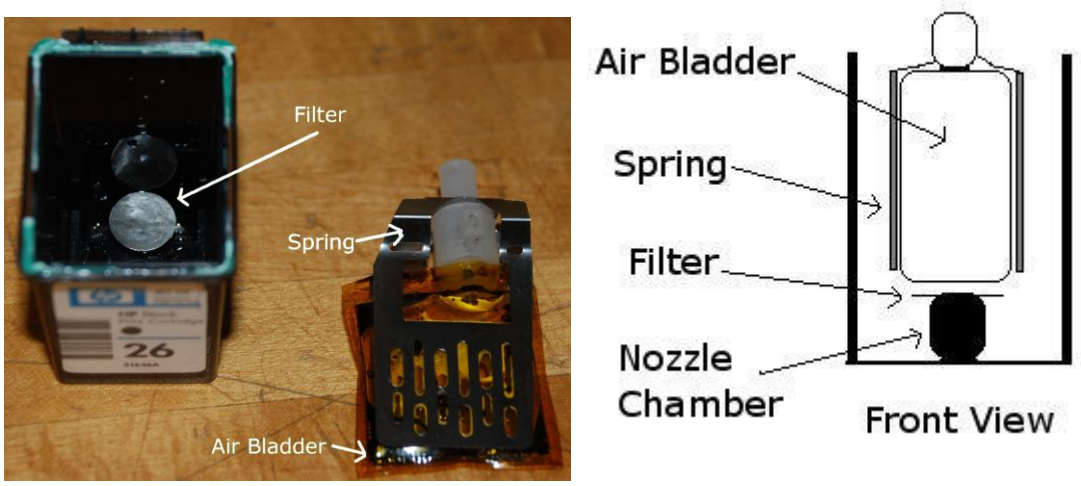

Figure 2-3 Internal Components of HP26 Cartridge and Cutaway View

The HP26 Cartridge was designed for the HP 500 series of printers. This allows the cartridge to be used in all the printers from this model line. The list of printers that use this cartridge was determined from the manufacturers packaging of the cartridge and is provided in Table 2-2.

Deskjet Plus		Deskwriter	Designjet	Officejet
400	520	510	200	300
420	540	520	220	330
500	550	540	600	350
500c	560	550		
510		560		

Table 2-2 List of Printers that use the HP26 Cartridge

Introduction to the HP 500 Series Printer

Overview of the HP 520C Printer

The HP520C printer has multiple components that compose the entire system. A functional decomposition of the system is shown in Figure 2-4. There is a microcontroller which acts as the master of the overall system that receives data through the parallel port connected to a PC. The microcontroller then controls three main subsystems: the head maintenance system, the motion system, and the driver board system that controls the firing of the HP26 cartridge. The printer functions by moving the print cartridge horizontally and the paper vertically so that the cartridge nozzles can be fired to deposit an ink droplet at any location on a sheet of paper. A page is printed in horizontal rows starting in the top left corner. The cartridge moves back and forth across the page and prints in both directions, i.e. bidirectional printing.

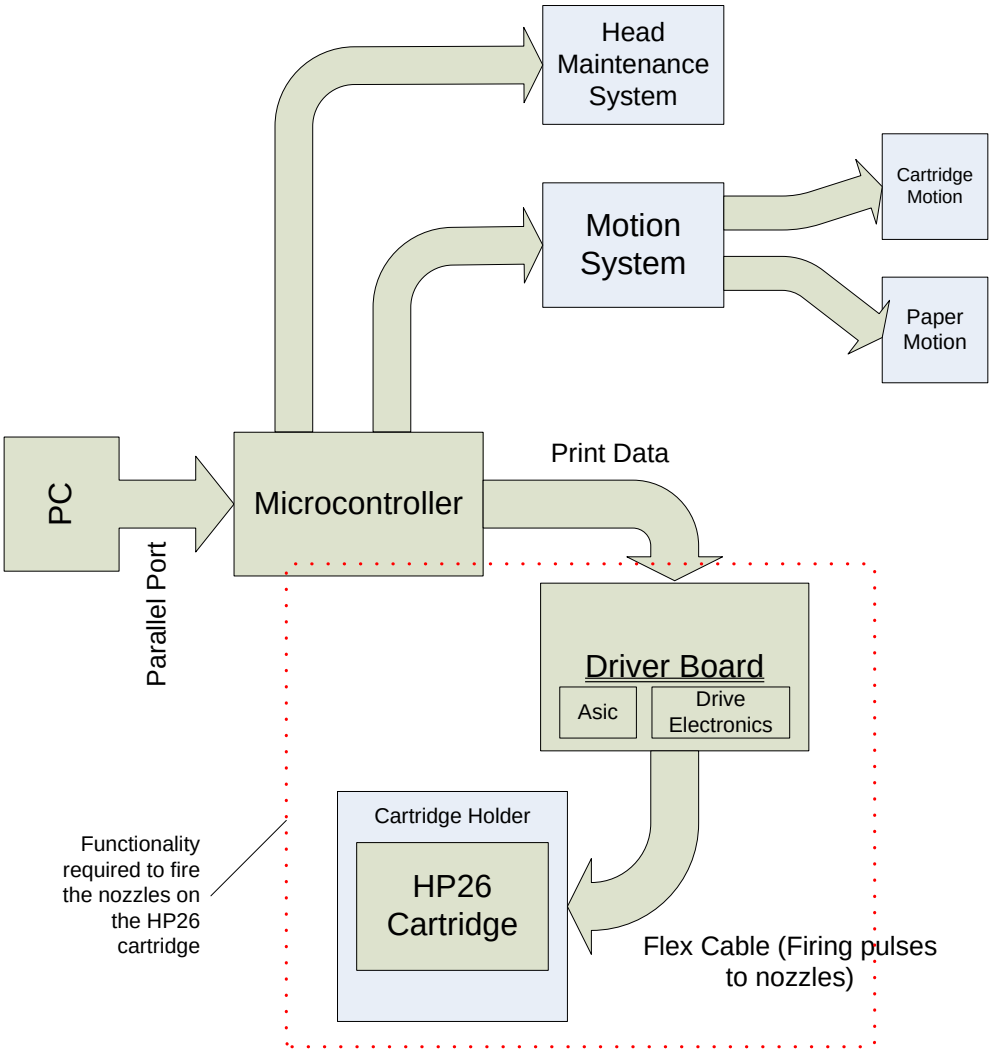

Figure 2-4 Components of the HP 520C's Printer Systems

The microcontroller is mounted on a PCB inside the printer. It formats the data for the driver board and controls all the motion in the system. The microcontroller receives the data through the parallel port from a PC that is transmitted in a proprietary format through the Hewlett Packard driver software

Components

HP 520C Driver Board

The Driver Board acts as an intermediate stage between the software running on the microcontroller receiving data from the PC and the HP26 cartridge. Various signals are required to fire the correct nozzle at the right time. The function of the driver board is to receive the instructions to fire a nozzle and generate the appropriate firing power signal for a nozzle in the printhead. The driver board, shown in Figure 2-5, consists of several different components necessary in the firing of the printhead. Among these components is a custom ASIC manufactured by Texas Instruments (Texas Instruments, Dallas, TX) TI 45AEJ8T, a supply capacitor from Nichicon (Nichicon Inc, Kyoto, Japan) 180 uF H9348, four resistors (14.7 ohms +/- 1% tolerance and ¼ Watts), two flex cable connectors, and a connector to main board of printer and are labeled in Figure 2-5.

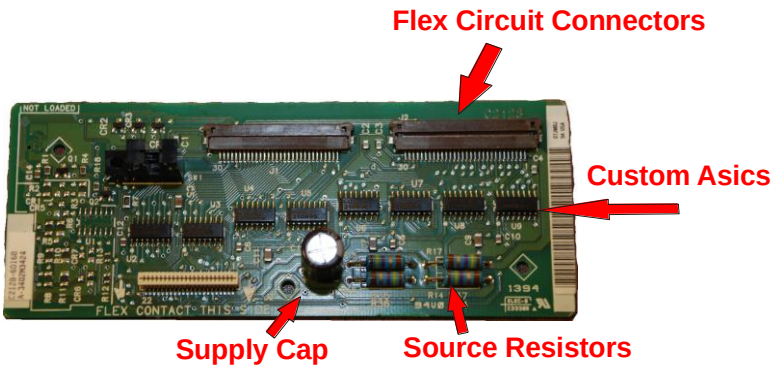

Figure 2-5 HP 520C Cartridge Driver

Flex Cables and Cartridge Holder

The driver board communicates to the print cartridge via cartridge holder through the flex connector pictured in Figure 2-6.

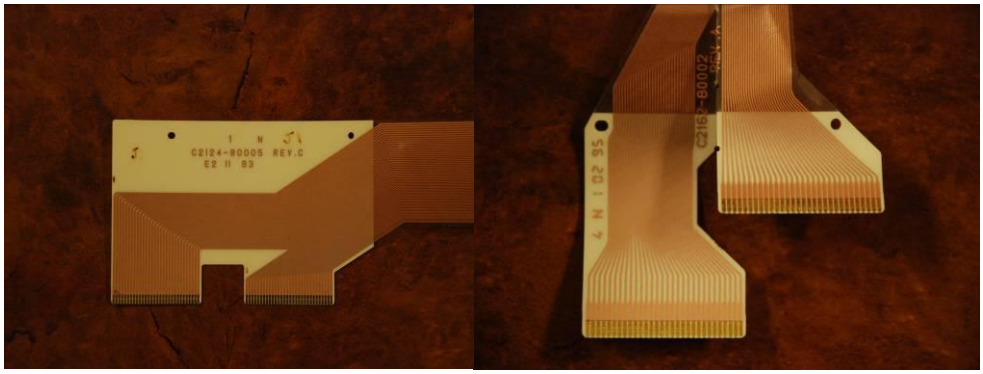

Figure 2-6 Flex Circuit Connectors

These cables provide a flexible cabling solution that allows the printhead to move freely and provide continuity to the print cartridge. There are flex cable connector geometries pictured in Figure 2-6 which were used in different models in the 500 series line. The connectors are 1 mm pitch size with 3 mm long contacts. The connectors are identical but the spacing between them is different. The cartridge holder provides physical support of the cartridge and the electrical connections to the cartridge.

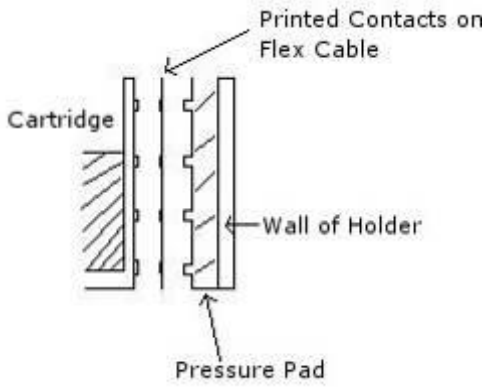

Figure 2-7 Cutaway View of Cartridge Holder

The components that constitute the electrical connection are depicted in Figure 2-7. A pressure pad behind the contacts maintains continuity.

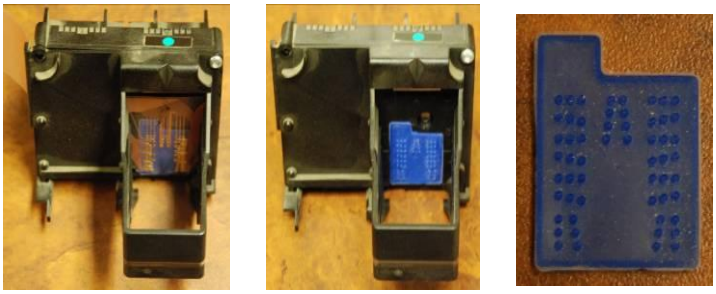

Figure 2-8 Print Cartridge Holder with Flex Circuit, Without Flex, and Pressure Pad

The print cartridge mates with the connections in Figure 2-8 via another flexible printed circuit that connects directly with the printhead of the cartridge. With this type of connection Hewlett Packard was able to provide removable cartridges with reliable electrical connections.

Head Maintenance System

The printhead maintenance system of the HP520C printer is consists of a service station with a stepper motor and a rubber plunger. Periodically the printhead will move to the service station, raise the plunger to the printhead height and create a parasitic pressure that is used to unclog the nozzles of the printhead. The components of the head maintenance system can be seen in Figure 2-9.

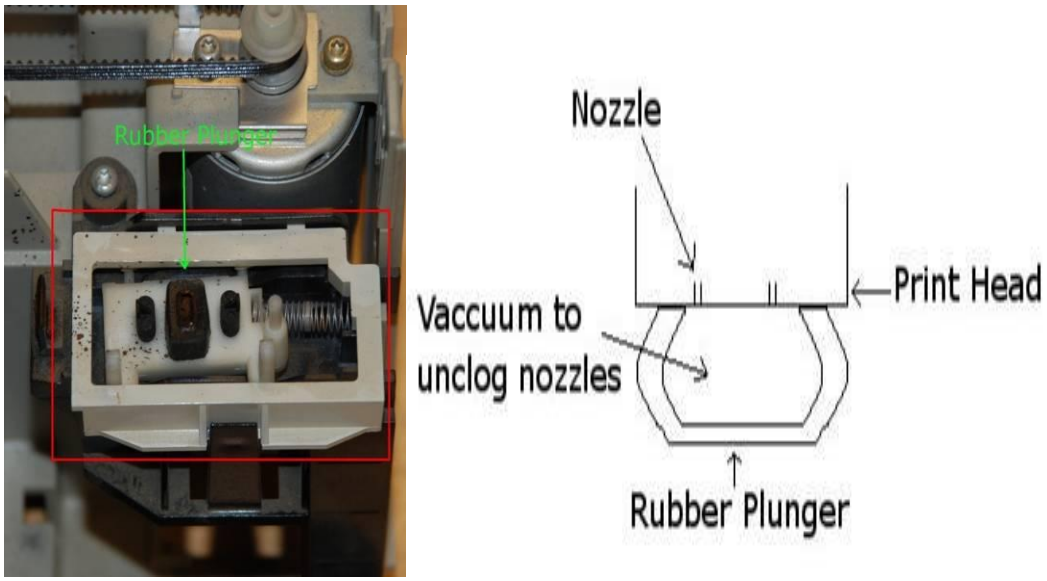

Figure 2-9 Head Maintenance Station and Cutaway view of Plunger

As the head travels over the gasket the printhead in Figure 2-9 the printhead compresses the plunger creating a pressure differential through a vacuum that unclogs the nozzle.

Motion System

The motion system of the HP 520C printer is composed into two subgroups. These two subgroups are the motion system for the printhead/carriage and the motion system that feeds the paper through the printer. The printhead motion system provides the lateral motion (the print direction) that allows the head to cover the entire width of the page while the paper motion system advances the paper through the printer (the paper direction). The printer uses a DC motor to move the printhead in the print direction. Feedback of the carriage position is provided by a linear encoder that is fixed along the direction of travel with a read head on the carriage. The encoder and the optical strip can be seen in Figure 2-11.We hypothesize that the DC motor provides faster speed in the

print direction than a stepper motor but needs closed-loop control in order to obtain accurate position control. The printhead motion system can be seen in Figure 2-10.

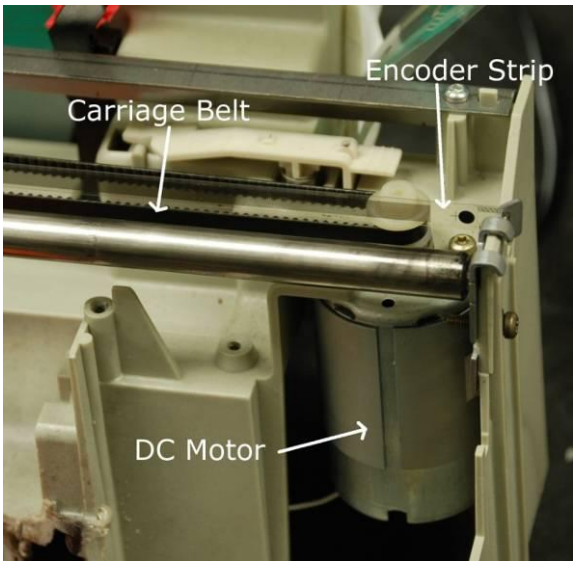

Figure 2-10 DC Drive of HP 520C Printer

The carriage is connected to the belt system that is driven by a gear on the DC motor.

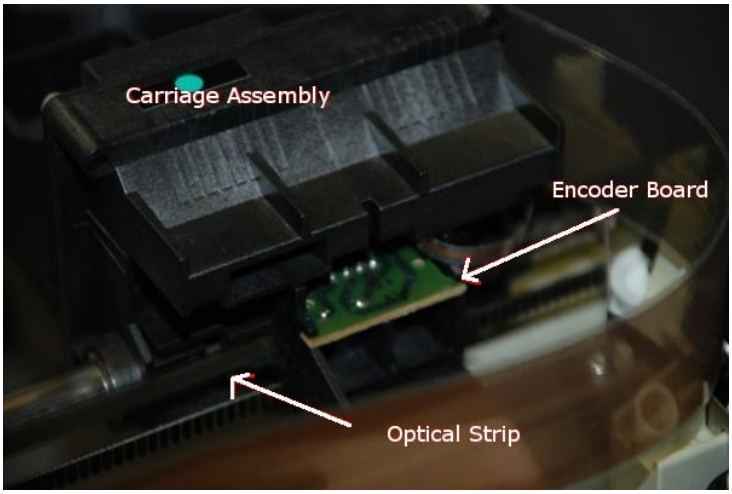

Figure 2-11 Encoder Assembly in HP 520C Printer

The paper motion system is comprised of a stepper motor and series of gears. The gears are used to spin a spindle that has wheels attached, which applies a force to the

paper with the wheels to advance the paper through the printer. The paper direction requires lower speed than the print direction, thus we hypothesize that an open-loop stepper motor is used to drive this subsystem. The stepper drive can be seen in Figure 2-12.

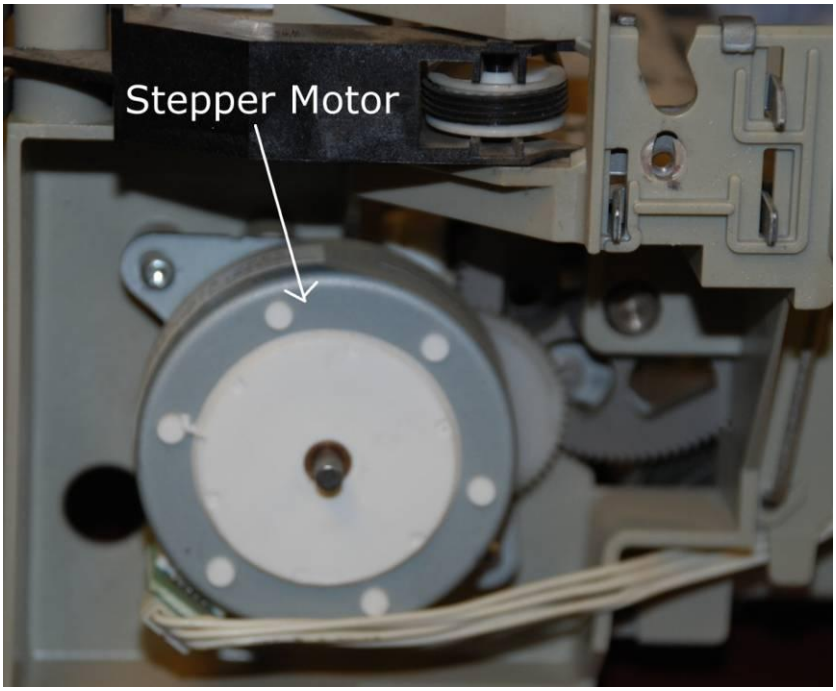

Figure 2-12 Stepper Drive for Paper Motion System

The stepper motor drives the gear attached to the spindle which is attached to the paper feeding wheels. These wheels can be seen attached to the spindle in Figure 2-13.

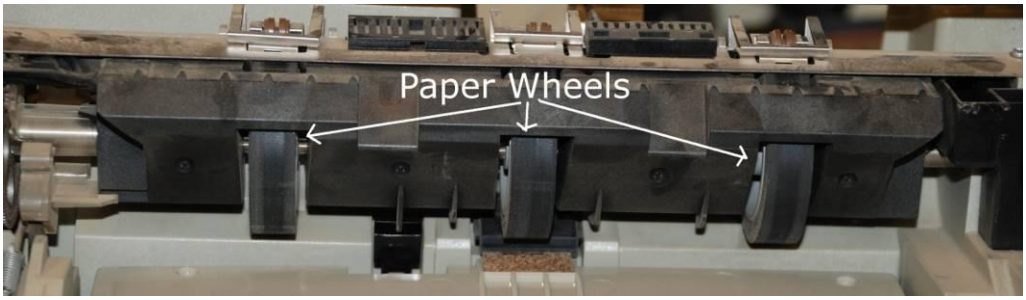

Figure 2-13 Paper Feed Mechanism

The wheels provide pressure against the paper and rotate, thus feeding the paper through the printer.

Plan for Reverse Engineering

With the main systems of the HP520C printer established, a plan for reverse engineering the components necessary for firing the print nozzles was developed. Our understanding of the HP520C printing system suggests that the functionality demarcated by the dotted line in Figure 2-4 is required to drive the printer. This functionality includes the driver board, cartridge, cartridge connections, and cartridge holder. The other systems including the microcontroller, motion system, and head maintenance system are not required for this specific aim. The individual components of these subsystems will now be analyzed in more detail through the examination of HP's technical journals, measurements, physical intuition, and known operation of select electronic components.

Operation of the HP 500 Series Printer

Review of HP Journals Regarding Design of HP 500 Series Printer

Hewlett Packard offers access to all of their technical journals in a public database. These journals provided valuable information in determining various parameters used in controlling the printing of the HP 500 series printers. The following is a summary of the information that was presented in these journals that was useful in quantifying the operation of the system.

The HP 26 series cartridges with integrated printhead were designed to operate at 300 dpi [12], i.e. every inch of printing will contain 300 dots or equivalently a dot every

85 microns in both the horizontal and vertical directions. This is the native resolution of the printer that results from the design of the printhead positioning system, i.e. the printer, and the printhead itself. The print frequency is 3.6 kHz, meaning a nozzle can fire 3,600 times per second [5]; this is the speed required to fire all the nozzles at the constant velocity that the printhead travels and achieve the 300 dpi resolution. The ink ejected from the printhead has a volume of 130 pL and the nozzles are approximately 50 microns in diameter [5]. The journals also provide some information as to the ink composition and the effects of viscosity as the ink is ejected from the printhead. In "Development of a high-resolution thermal inkjet printhead", William Buskirk claims that if the viscosity of the ink decreases then the overall fluid damping of the dynamics of the drop being ejected from a nozzle will negatively affect the performance of printing. Also the meniscus of the bubble oscillates about the equilibrium point of the nozzle, thus causing deformations in the ink drops being ejected [5].

In The HP Journal, "Data to dots in the HP DeskJet Printer", the purpose of staggering the individual nozzles on the printhead as seen in Figure 2-14 is explained as a solution to the delay caused from only printing four nozzles at once [9].

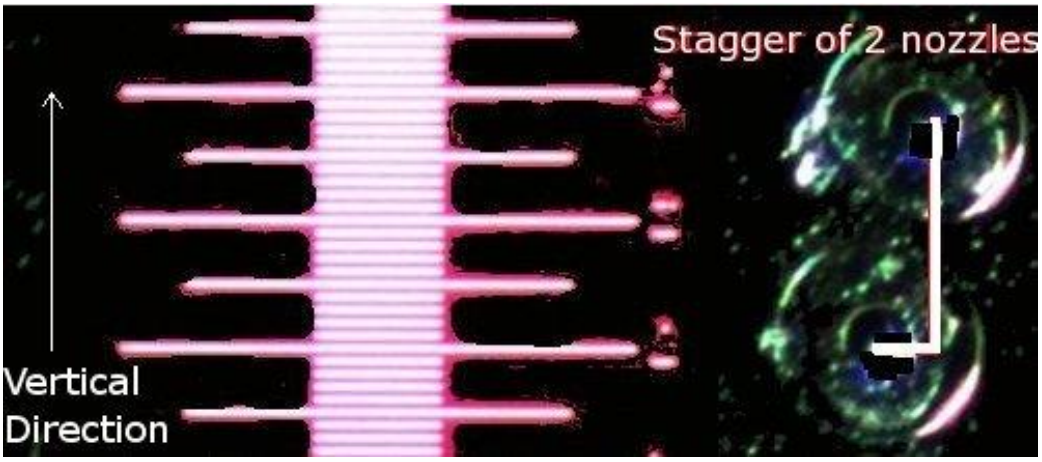

Figure 2-14 Example of a Staggered Nozzle, Major Divisions of 100 Microns

The 3.6 kHz frequency at which the printer fires directly translates into a time period of 139 microseconds to print all of the 50 nozzles (2 columns of 25) on the printhead. This printing period is further divided into thirteen periods and four nozzles are fired in each of these periods. [9]. All of this data can be seen in Table 2-3. HP chose this method to account for the time delay associated with the offset columns and the time to print all fifty nozzles which arise while printing at a constant velocity.

	Deskjet 500 Series
Resolution	300 dpi (85 microns)
Number of Nozzles	50
Frequency	3.6 kHz
Drop Volume	130 pL

Table 2-3 Properties of HP 500 Series Printer

The HP Journals also provide some insight into the purpose of a custom ASIC, Texas Instruments part number 45AEJ8T, used on the Driver Board. First the chip acts as a decoder to select which nozzle in the cartridge to fire [7]. Secondly, the ASIC has a 25

bit wide, 20 bit long shift register to allow for the second column of nozzles to print in the proper x location in the printers coordinate system by delaying the trailing column with the appropriate amount of no fire commands to account for the horizontal distance between columns [9]. The final functionality is that it adjusts the pulse width relative to the temperature coefficient of the BJT's saturation voltage to maintain constant energy to the printhead [7].

The amount of energy delivered to the nozzle's thermal resistor varies with respect to the temperature of the resistor, since the resistor's resistance varies with temperature. Two solutions are proposed [7] to solve the problem of energy variation. The first is the addition of a resistor in series with the printhead thermal resistors to counter the variation of resistance experienced as heating occurs [7]. This works because the added resistors are external to the print cartridge and are not experiencing dramatic fluctuations in temperature. Thus, the change in the amount of current delivered to the print cartridge remains small compared to the overall resistance. The second solution in [7] is monitoring the saturation voltage of the transistor as temperature changes and adjusting the firing pulse width based upon the amount of temperature change monitored. Thus the energy delivered to the printhead is compensated by adjusting the duration of the pulse driving the printhead accordingly. This ability is built into the custom ASIC, through the monitoring of the voltage drop across the saturated transistor.

Measured Operation of the HP 520C Series Printer

Since most of the parameters of the HP 500 series printer were given in the literature, few measurements were required to fully understand the operation of the 500

series of printers. The most interesting signal in the 520C printer is the waveform that is applied to the nozzle resistor to eject a drop. The waveform was measured at the source resistor shown in Figure 2-5 on the driver board and is shown in Figure 2-15.

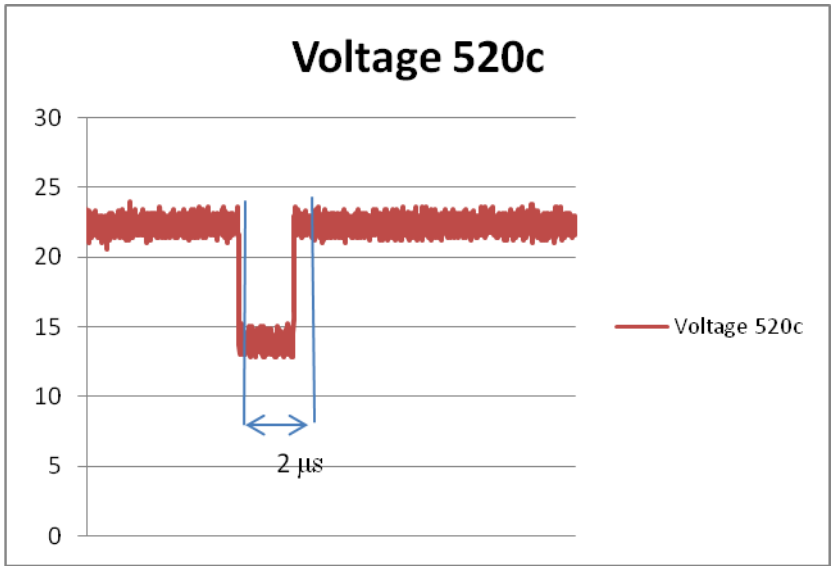

Figure 2-15 Voltage Drop across a HP26 Cartridge Nozzle

This experiment was repeated several times with the 520C printer. The overall result was a fourteen volt drop across the printhead. It will be shown later this value includes the collector-emitter saturation voltage of a BJT used to select the nozzle firing. The firing pulse lasted for 2 microseconds.

The energy dissipated in the printhead is calculated via Equation 2-1,with R being the resistance of the print nozzle, as

$$E = \int_0^T \frac{V^2}{R} dt \rightarrow E = \frac{V^2 T}{R}. \quad (2.1)$$

Using this equation for energy and the measured values, the estimated energy supplied to a nozzle is 12.25 μJoules. The result can then be compared to the equation given in the HP Journal [7].

$$I \cong \frac{(V_s - V_{sat})}{R_{tf} + R_{source} + R_{cap}} \quad E = I^2 R_{tf} T \qquad (2.2)$$

Where V_s is the source voltage, V_{sat} is the saturation voltage of the BJT, R_{tf} is the thermal resistor in the nozzle, R_{source} is the added source resistor, and R_{cap} is the series resistance of the capacitor placed on the V_s supply rail. The parameters used to calculate this are given in Table 2-4 and were obtained through measurement.

V_s	24 V	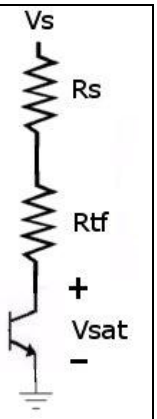
V_{sat}	1.45 V	
R_{tf}	32 Ω	
R_{source}	14.7 Ω	
R_{cap}	2.7 Ω	
t	2 μs	

Table 2-4 HP 500 Parameters for Energy Calculation

Using the equation that HP provided for the actual system, the energy was determined to be 13.34 μJoules. This is an error of eight percent in energy delivered to our model.

Modeling HP520C Operation

Model of HP26 Cartridge

Review of the literature and physical examination of connections on the driver board led to the proposal of a model for a single nozzle in the HP26 cartridge shown in

Figure 2-17. This is due to the structure of the print cartridge itself, where each nozzle is modeled as a resistor and are joined into quadrants that are fed with a four common inputs. The groupings of the nozzles are also shown in Figure 2-16 and are important information in regards to the geometry of the printhead. The model was verified by touching a Fluke Model 179 multi-meter to the pins of the cartridge. Fifty measurements were taken on several cartridges and the nominal resistance was found to be 30.7 ohms with a standard deviation of 0.225 ohms.

Figure 2-16 Close-up of HP26 Quadrants at 10x Magnification

The address must be selected for the proper nozzle in each four quadrants. These are set from the microprocessor on the main board of the printer and go directly to the decoders in the custom ASICS. Each quadrant has two ASICS, therefore each ASIC must contain a 3x8 line decoder to be able to address every nozzle in the quadrant of nozzles. This being the case each decoder must have three enables, one used to combine the decoders into a 4x16 line decoder, one to transmit firing data, and one for a clock input provided by the

microprocessor at the firing frequency of 3.6 kHz. The firing waveform has been shown previously in the chapter and will be discussed later in comparison to the custom systems firing waveform. These are all the signals required to fire a nozzle on the HP 500 series printer. This leads to the parallel nature of the model for the entire cartridge which can be seen in Figure 2-17.

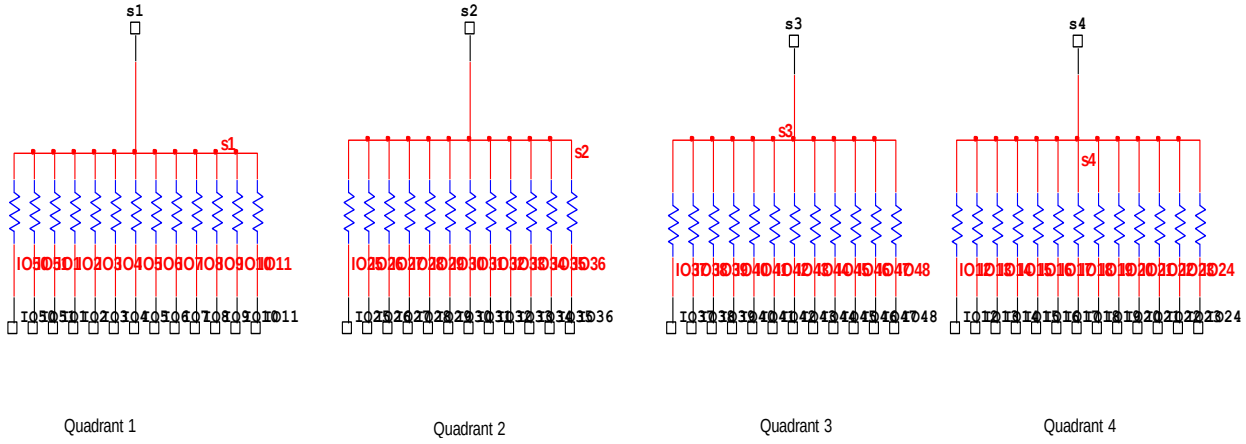

Figure 2-17 Model of HP26 Cartridge

Model of HP520C Printing System

The HP520C Printing system is composed of the driver board and its connections to the HP26 cartridge. The internal decoders provide a path to ground for the thermal resistor built into the cartridge, thus allowing the printer to fire a drop. The cartridge is connected to a transistor inside the ASIC via a flex cable circuit, of which two types were found in the 500 series printers.

With the decoder architecture on the driver board and the knowledge of the nozzle groupings into four quadrants, a model can be proposed for the nozzle drive components located on the driver board.

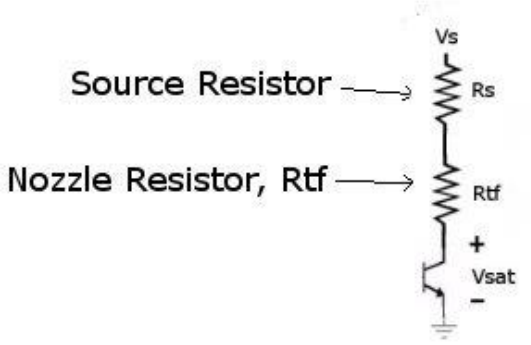

Figure 2-18 Model of Single Nozzle in Context of Drive Electronics

In the model in Figure 2-18, R1 is the added source resistor on the Driver Board and R2 is the resistance of a single nozzle inside the printhead. This model was expanded to consist of a model for the entire cartridge. The knowledge about the decoder structure of the custom ASIC, and about the groups of resistors inside the cartridge led to a four-group, parallel structure comprised of the single nozzle model and is shown in Figure 2-19.

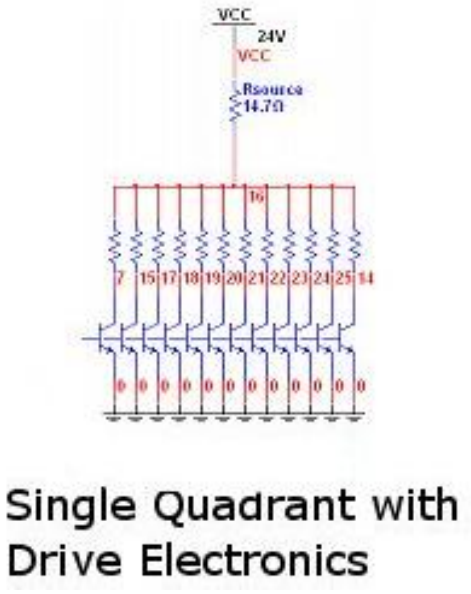

Figure 2-19 Single Quadrant of HP 26 Cartridge

The model proposed in Figure 2-19 was simulated and verified using National Instrument Multisim version 10.0 to match the measurements shown in the previous section. In the source resistance is shown inserted into the model at the common node for the individual quadrants and the nozzle resistances are shown connected to the collector of a BJT simulating the connection to the custom ASIC. When the encoders built into the custom ASIC select a nozzle they drive a transistor into saturation, thus providing a path to ground potential. The ASIC may use FETs rather than BJTs.

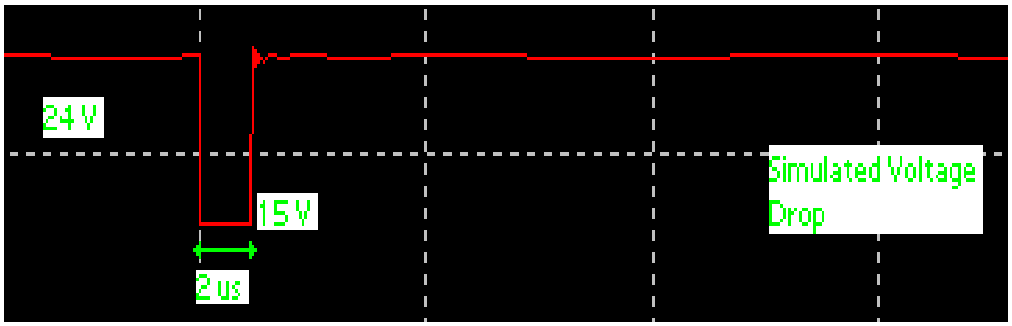

Figure 2-20 Simulation Waveform

This simulation was repeated for each nozzle in the model, each obtaining the same result which has the same voltage drop as that measured in the physical system (Figure 2-15). The similarity of the measured and simulated waveforms, Figure 2-15 and Figure 2-20, confirms the validity of the model of the HP26 Cartridge and the drive circuitry.

HP26 Cartridge Interface

The result of the above work is that the driver board could be replaced by custom electronics that reproduces the correct power waveforms. It was noted that the connection technology between the cartridge and the cartridge holder could not easily be reproduced. Thus, stand-alone use of the cartridge will include the cartridge holder and the flex

cables. The connection of the HP26 Cartridge and printhead to the printer through the flex cables is now described. The HP26 cartridge has fifty-six connections to the print driver board through a flex circuit on the back side of the cartridge as seen in Figure 2-21.

Figure 2-21 Flex Circuit of the HP 26 Cartridge

These connections provide four source points of 24V DC for the firing waveform to enter the cartridge and fifty connections to provide return paths for each individual nozzle as shown in Figure 2-19 and two connections for print cartridge identification. Figure 2-22 shows the two compression headers that connect the flex cables to the cartridge holder. It provides a pin identification of the pin connections on the printer board where the flex cable is inserted with the contacts on the bottom. Figure 2-23 provides a map that assigns cartridge inputs to pin members.

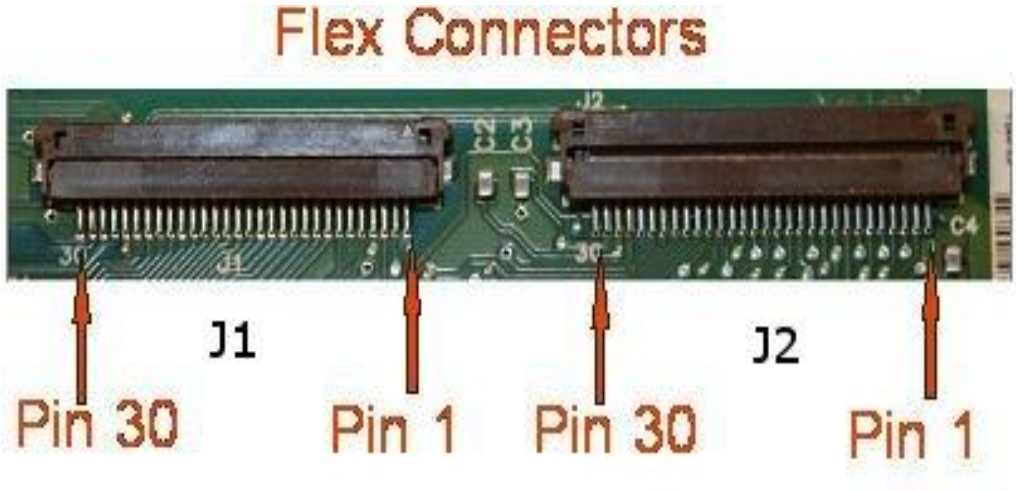

Figure 2-22 Close-up of Flex Connectors

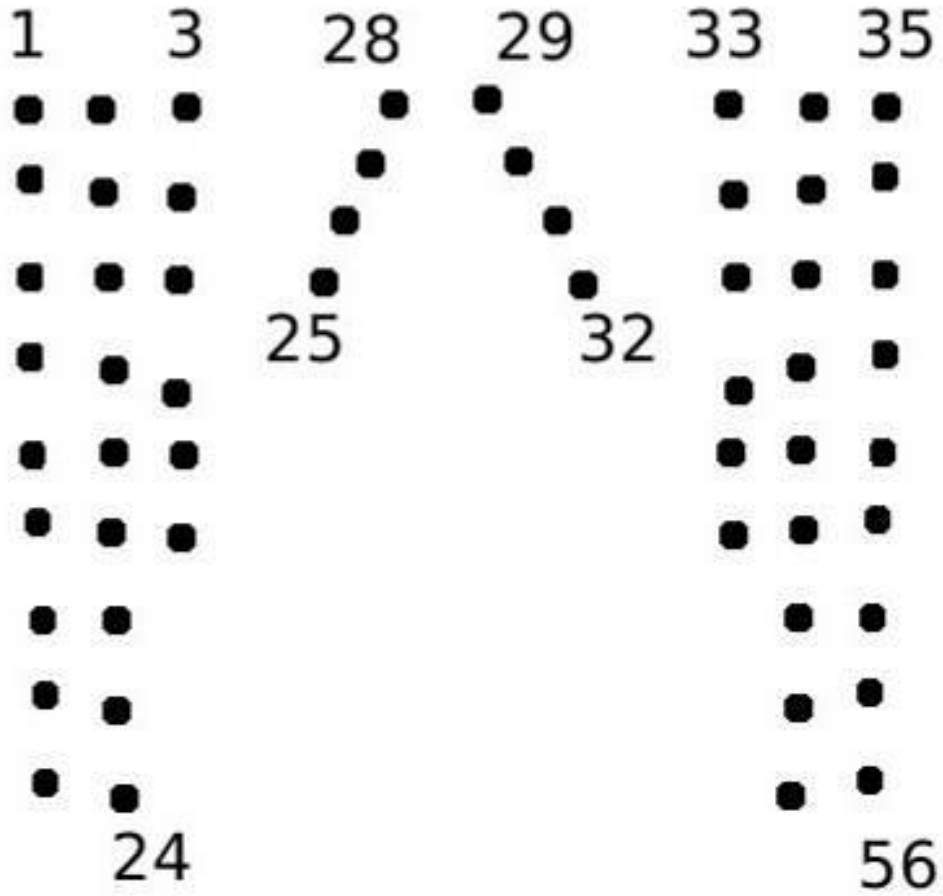

Figure 2-23 Map of Print Cartridge Contacts

Cartridge Pin #	Connector	Connector Pin	Cartridge Pin Function
1	J1	5	Group R3
2	J1	4	Group R3
3	J1	3	Group R3
4	J1	7	Group R3
5	J1	8	Group R3
6	J1	6	Group R3
7	J1	10	Group R3
8	J1	9	Group R3
9	J1	11	Group R3
10	J1	12	Group R3
11	J1	13	Group R1
12	J1	14	Group R1
13	J1	16	Group R1
14	J1	15	Group R1
15	J1	17	Group R1
16	J1	18	Group R1
17	J1	19	Group R1
18	J1	20	Group R1
19	J1	22	Group R1
20	J1	21	Group R1
21	J1	24	Group R1
22	J1	23	Group R1
23	J1	26	Source for R1
24	J1	25	Group R1
25	J1	2	Group R3
26	J1	1	Cartridge ID
27	J2	30	Group R3
28	J2	28	Source for R3
29	J2	29	Source for R2
30	J2	27	Group R2
31	J2	26	Cartridge ID
32	J2	25	Group R2
33	J2	24	Group R2
34	J2	23	Group R2
35	J2	22	Group R2
36	J2	21	Group R2
37	J2	19	Group R2
38	J2	20	Group R2
39	J2	16	Group R2
40	J2	18	Group R2
41	J2	17	Group R2
42	J2	13	Group R4
43	J2	14	Group R4
44	J2	15	Group R2
45	J2	10	Group R4
46	J2	12	Group R4
47	J2	11	Group R4
48	J2	7	Group R4
49	J2	8	Group R4
50	J2	9	Group R4
51	J2	6	Group R4
52	J2	5	Group R4
53	J2	4	Group R4
54	J2	3	Group R4
55	J2	2	Group R4
56	J2	1	Source for R4

Table 2-5 Map of HP26 Cartridge to Flex Cable Connectors

Table 2-5 provides the mapping of each connection on the HP26 Cartridge to the headers. These connections are in terms of the pins labeled in the map of the flex circuit on the print cartridge in Figure 2-23 and the flex cable pin connections on the driver board given in Figure 2-22. With this mapping the print cartridge connections can be understood in the context of the HP 500 series printer. The groups were assigned in Table 2-5 according to which source resistor fed the common voltage to that specific group of resistors. This still did not allow for the determination of which nozzle on the printhead matched to which contact on the cartridge. This knowledge would be determined using the first cartridge driver prototype system.

Conclusion

With the reverse engineering of the print subsystem complete, we now have the basis to build a custom printing system as shown in Figure 2-24. A custom motion system will be employed as well as custom electronics that simulate the electronics from the HP 500 series printers. The custom electronics will be controlled via a software interface to simulate the role of the HP 500 series microcontroller. The only parts necessary from the HP 500 series printer will be the flex cable system and cartridge holder system.

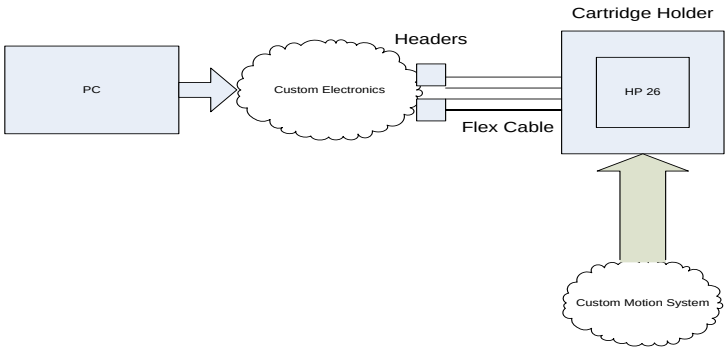

Figure 2-24 Custom System

CHAPTER THREE
CUSTOM HP26 SERIES CARTRIDGE DRIVER

The motivation for designing a custom driver for the HP26 cartridge lies in the need to have a system where all the parameters to fire the nozzles in the HP26 cartridge are accessible to the user, in contrast to the HP 500 series of printers where the firing parameters and timing are outside the user's control. The goal of the research described in this section is to design and build a robust digital circuit that can accurately control the HP26 series cartridge described in the previous chapter. The end user of the hardware will be able to directly request that a specific nozzle in the printhead fire to eject a droplet. The overarching aim is to build a HP26 cartridge driver such that it can be incorporated into an automated printing system.

Design of the Custom HP26 Cartridge Driver

Design Approach

A combined top-down/bottom-up approach was taken to generate the main components of the cartridge driver system proposed in Figure 3-1. The existing cartridge holder and flex circuit connectors from an HP500 series printer are reused in order to limit the amount of mechanical design needed to develop a working prototype. The user interface and as much control logic as possible is implemented using a PC equipped with Matlab/Simulink (Mathworks Inc, Natick, MA), Wincon 5.1 (Quanser, Ontario, Canada), and the Quanser Q8 hardware (Quanser, Ontario, Canada). The PC-based controller was chosen because it provides a rapid prototyping environment. A minor constraint placed

on the design of the custom driver board was to minimize the area of the circuit board in order to ease physical integration into the final system and to minimize the cost of having the board manufactured. In Figure 3-1 the role of the custom driver board can be seen in the overall functional decomposition of the proposed system where the dotted box indicates the functionality of the Driver Board.

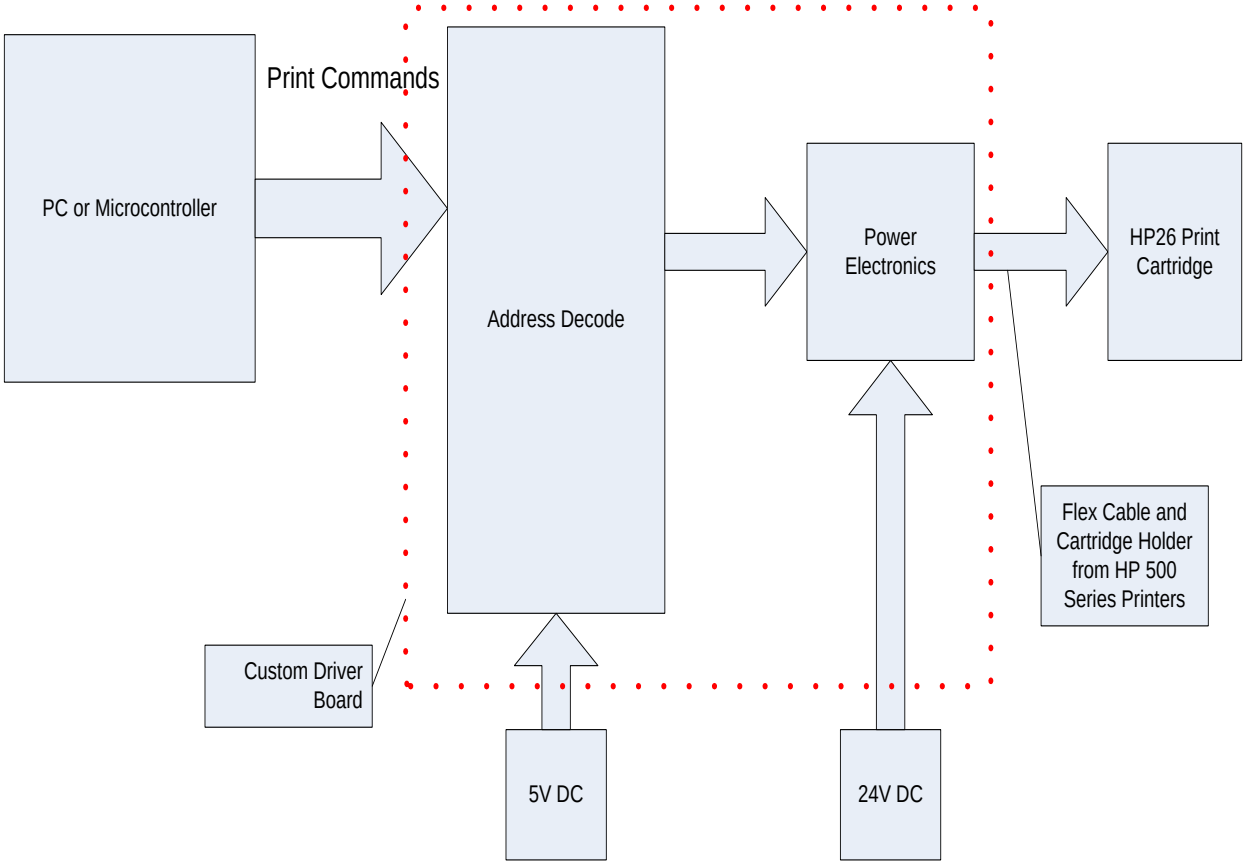

Figure 3-1 Block Diagram of Proposed System

Address Decoding Subsystem

The function of the custom ASIC used in the original HP 500 printer suggested a further decomposition of the driver board functionality as shown in Figure 3-2,

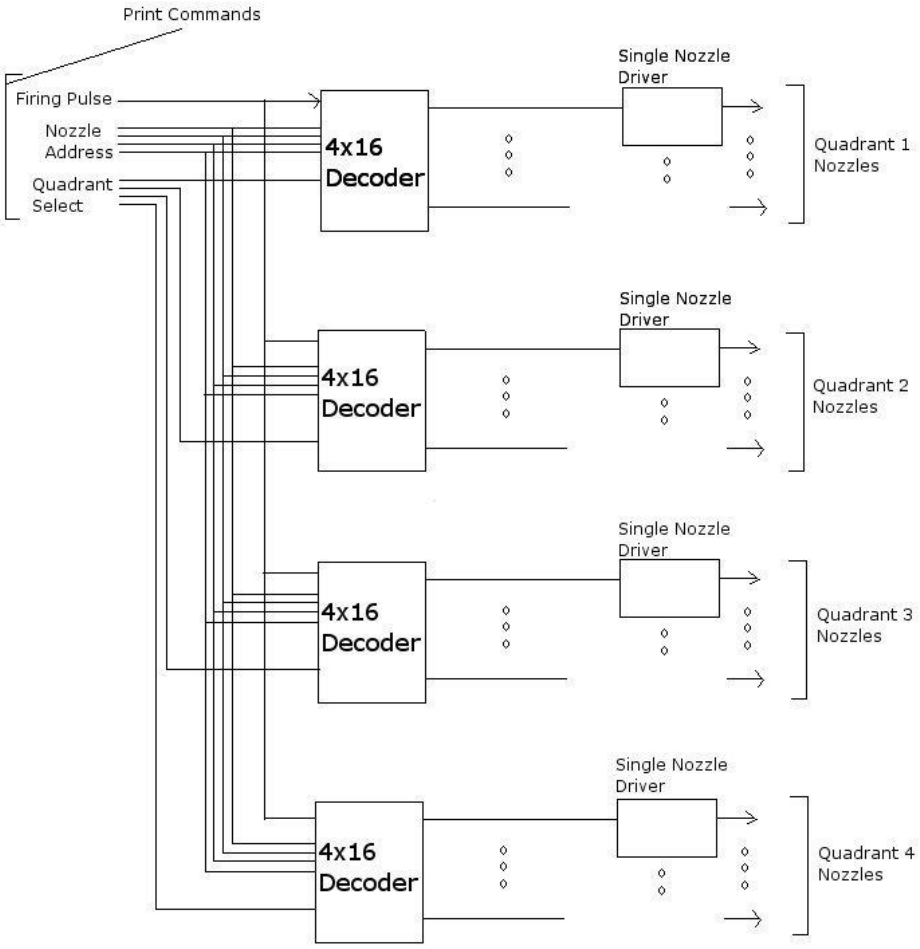

Figure 3-2 Decomposition of Driver Board

since the ASIC acts like a decoder that selects which nozzle to fire in the specific quadrants.

Design of a 4x16 Decoder

Decoders are commercially available that provide 4 address lines and 16 outputs, however the outputs of this class of decoders are initially logic level high and would therefore need additional inverting logic to interface with the proposed power electronics.

Therefore the decoders chosen for the custom driver board were the 74HC238 family of 3x8 line decoders (STMicroelectronics, Geneva, Switzerland). This line of decoders provides for the selected output to go high when enabled, which can then be used to drive the input base of the Darlington pair in the next stage. The published switching time is 15 ns. Two decoders must be used address a quadrant of nozzles (13 nozzles max). The three address lines are used to provide the lower three bits of the nozzle address and one of the three enables on the chip (~G2B) is used to add an extra high bit to the address line. The enable ~G2B is active low, so the resulting 4x16 line decoder had a structure that can be seen in Figure 3-3.

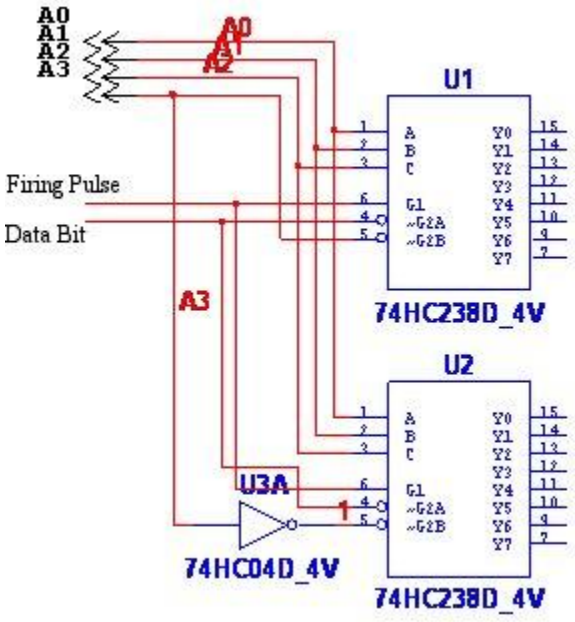

Figure 3-3 Two 3x8 Decoders Operating as a 4x16 Decoder

When A3 becomes high it selects the second decoder, thus providing the higher byte of the 16 lines through the use of the inverter that enables the second decoder.

To create the desired waveform to drive the printhead, the remaining two enables G1 and ~G2A on the decoders are used, note that ~G2A is inverted at the input. A square wave with the pulse width required to drive a nozzle is applied to the high active enable G1. The firing pulse is not passed to the addressed nozzle G2A is enabled. The combination of G2A enabled (active low) with the firing pulse on G1 sends the firing pulse to the addressed nozzle. When the firing pulse is 5V and the second enable G2A is ground, then the selected output receives a 5V pulse that lasts the duration of the firing pulse. This 5V pulse drives the power electronics which in turn fire the cartridge nozzle. The firing pulse is sent to every decoder regardless of quadrant. The second enable, G2A, selects the quadrant(s) that will fire.

Figure 3-4 presents an example of a row vector [0 0 1] to be printed. Recall that the data is inverted at G2A so this should print two drops.

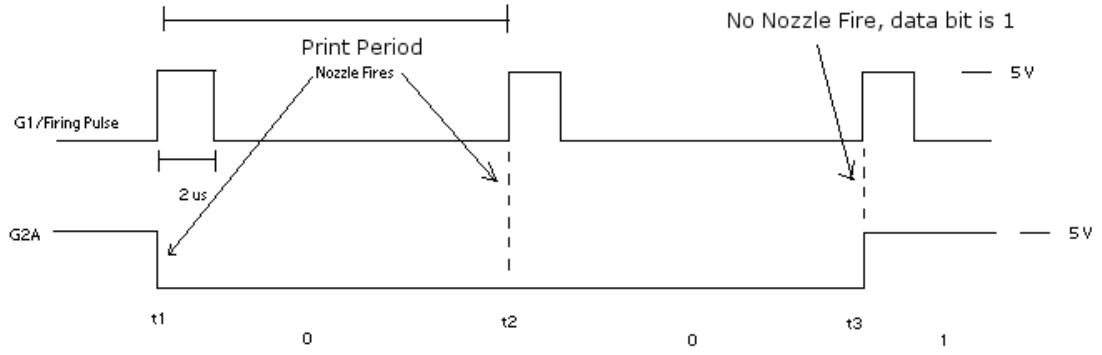

Figure 3-4 Decoder Enables During a Print

Therefore two drops will be ejected from the printhead nozzle addressed by the quadrant select line and the three address lines. The print period for the firing pulse is set by the rate at which the PC or microcontroller can update the address, print data, and print firing

pulse. The expected rate for the initial prototype is 1 ms; however; the minimum printing time allowed by the Driver Board will be dictated by the switch time of the power section and the duty cycle of the nozzles. The firing pulse width should match that of the observed waveform in Figure 2-15 and will be compared to it later in the chapter.

Nozzle Power Subsection

The next step in designing the cartridge driver was selecting a transistor that would be used as a switch to connect the nozzle resistor to ground potential. Since the transistor must sink 484 mA of current, a solution was sought for this level of current. This came in the form of the Toshiba TD62003 which is a 7 channel Darlington-pair high-current transistor array. The maximum current of 0.5 A for this package is close to the amount drawn in firing a nozzle but should not be an issue due to the short duration of the pulse. Since there are 7 channels per chip, two are needed to cover a single 12 or 13 nozzle quadrant of the printhead. The model that comprises a single channel of the TD62003 is shown in Figure 3-5 and is reproduced from the Toshiba datasheet.

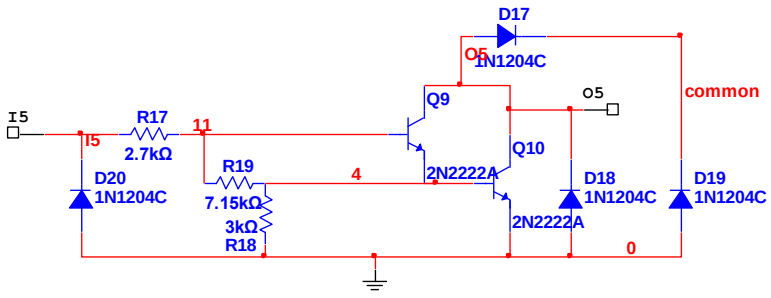

Figure 3-5 Darlington Transistor Pair with Input I5 and Output O5

The response time of these drivers is 0.1 microseconds, well within the time frame needed for this project.

With the main driving components of the hardware for the driver board determined, the remaining components of the output circuit in Figure 3-7 were selected. The source resistors were chosen based upon the resistors used in the HP 520C printer; however, the value of 14.7 ohms ¼ watts could not be obtained through standard suppliers so instead a 13.7 ohm ¼ watt resistor was used. To study the sensitivity of the energy supplied to the nozzle to variations in the source resistance, the equation for energy in Equation 2-1 was modified to include a varying source resistance R_{source} and is provided as

$$\frac{V_{source}R_{nozzle}}{R_{nozzle}+R_{source}}=V_{nozzle} \text{ and } E_{nozzle}=\frac{V_{nozzle}{}^{2}T}{R_{nozzle}} \tag{3.1}$$

which can be combined to yield

$$E_{nozzle}=\frac{R_{nozzle}}{(R_{nozzle}+R_{source})^{2}}V^{2}{}_{source}T\,. \tag{3.2}$$

Note that V_{sat}=0V was used in deriving 3.1 from 2.1. The source resistance was varied from 2 to 50 ohms in Equation for 3-2 and the results are plotted in Figure 3-6.

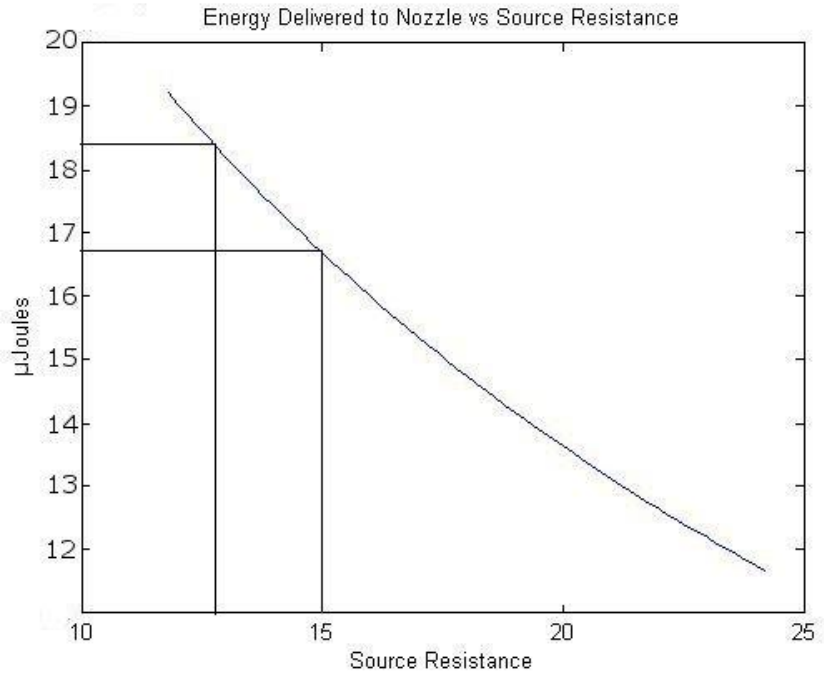

Figure 3-6 Sensitivity of Energy Delivered to Nozzle to Source Resistance

The energy delivered to the print nozzle varies two µJoules over the range of 13 to 15 ohms. This small amount of energy variation is not enough to severely affect printing performance as pulse-width tests of the driver board will later show.

The only component left to specify was the connector solution for the flex cable to the cartridge holder. Determining the proper flex circuit connector for the print cartridge connection required measuring the flex cable, determining which side the contacts needed to be on and the method of securing the cable into the connector. The width of each male connector on the flex cable was 31 mm, with a pitch size of 1 mm (the pitch size is the distance between contacts). Since the printer used connectors with contacts on the bottom this was the style of connector required. The connector found to satisfy these criteria was the SLW30R (FCI, Versailles, France). The connector provides

a slide that uses pressure when engaged to lock the flex cable into position. The other connectors used for input signals were simple header strips.

Prototype Design

Printed Circuit Board Design

Design and layout of the printed circuit board was performed using the Circuit Design Suite Version 10.0 (National Instruments, Austin, TX). The design was done using the schematic capture program Multisim, a part of the Circuit Design Suite, which has a simulation package that allows for verification of a circuit before designing a PCB. The simulation model for the Darlington-pair driver from Toshiba was created using the model information from the datasheet. The remaining components had existing simulation models in the software package. One of the four quadrants of the schematic/simulation model is shown in Figure 3-7.

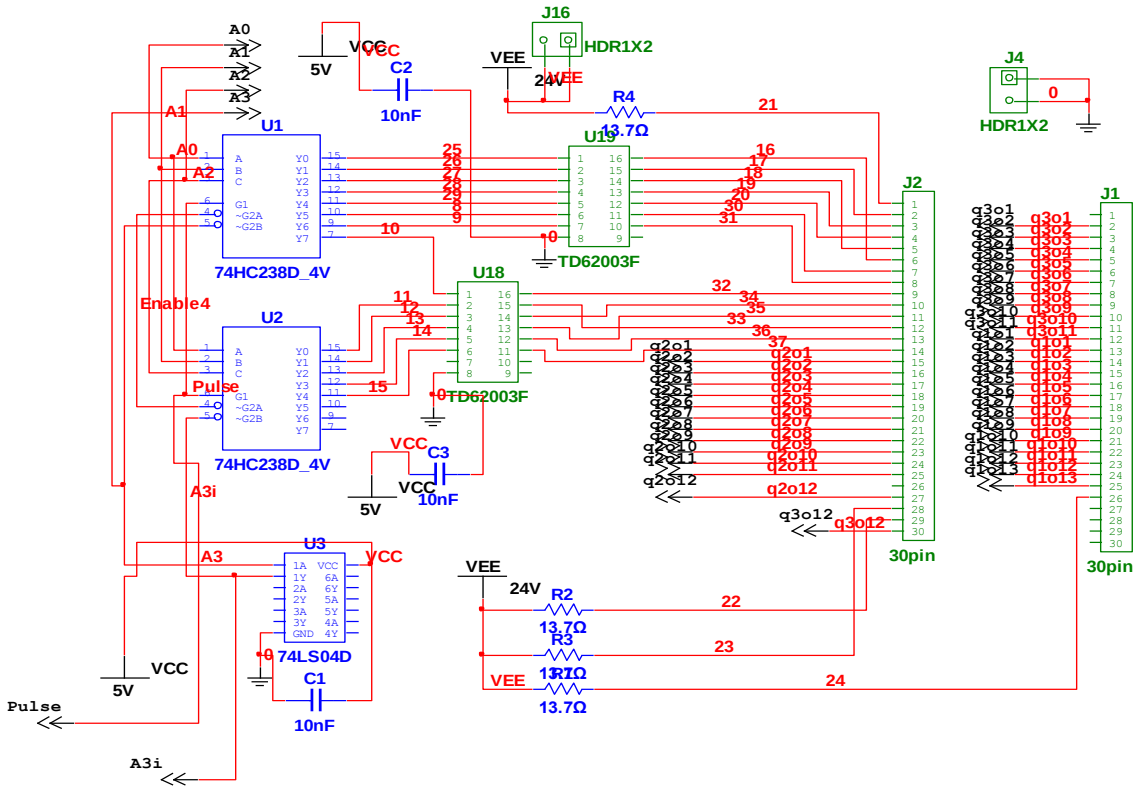

Figure 3-7 One Quadrant of Driver Board Schematic (Multisim)

U1 and U2 in Figure 3-7 are the two decoders for this quadrant of nozzles, U3 is the 7404 inverter used to select which decoder is enabled, and U18 and U19 are the Toshiba Darlington drivers. G2A is has a virtual connection to another page of the schematic as do the connections on J1 and J2. This schematic was repeated three more times to yield a circuit that was able to drive all the nozzles of the HP26 series cartridge. A bill of materials for the PCB is listed in Table 3-1.

Quantity	Description	RefDes	Package
1	HDR1X12	J3	Generic\HDR1X12
3	HDR1X2	J17, J16, J4	Generic\HDR1X2
8	74HC238D_4V	U14, U15, U10, U11, U2, U1 , U5, U6	IPC-7351\SO-16
8	TD62003F	U16, U17, U12, U13, U8, U9, U18, U19	IPC-7351\SO-16
9	CAPACITOR, 10nF	C8, C9, C6, C7, C4, C5, C3, C2, C1	Generic\0603
4	RESISTOR, 13.7Ω	R1, R3, R2, R4	Generic\RES1206
2	30pin SLW30R	J1, J2	Generic\SLW30R2
1	74LS04D Inverter	U3	IPC-7351\SOIC-14

Table 3-1 Bill of Materials for Driver Board

Once the schematic was captured, inputs were simulated in the software package to fire the nozzles, represented by 32 ohm resistors. This data was used to validate the nozzle voltage waveform that would be used to fire the cartridge in the proposed design. The simulated output for one nozzle is shown in Figure 3-8 where the input pulse triggers current in the nozzle resistance and hence a drop in the nozzle resistance voltage.

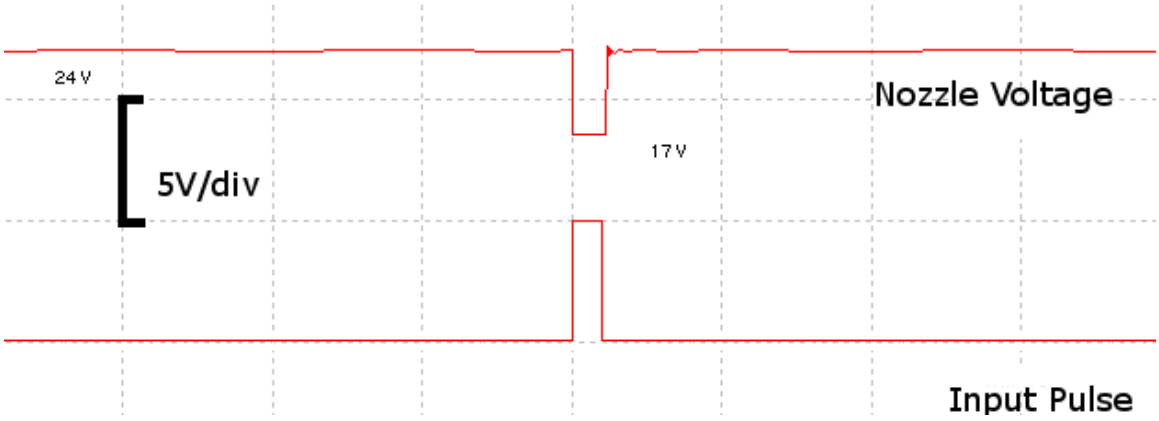

Figure 3-8 Simulated Voltage Drop from Design

The simulation suggests that the proposed Cartridge Driver circuit will provide an adequate waveform to successfully print with the HP 26 series cartridge.

Software and PC Setup

To control the prototype Cartridge Driver board a PC was configured with MATLAB 7.1 and Simulink 6.6 (Mathworks Inc, Natick, MA). The Q8 data acquisition card from Quanser was installed in a PCI slot in the PC, and WinCon 5.1 was installed (Quanser Inc, Ontario, Canada). The Simulink package is integrated into the control and operation of the Q8 by compiling Simulink models into executable programs that run in real time under WinCon, therefore the Driver Board will be controlled using a Simulink model. The (PWM) output on the Q8 is used to create the firing pulse. Since the frequency of the print commands (address and data) are limited by the update rate of the controller implemented in the real-time Simulink model set at 1 kHz, a 2 microsecond pulse can only be generated every millisecond since only one firing pulse can be used during each update of the controller. The Simulink software used to fire a drop can be seen in Figure 3-9.

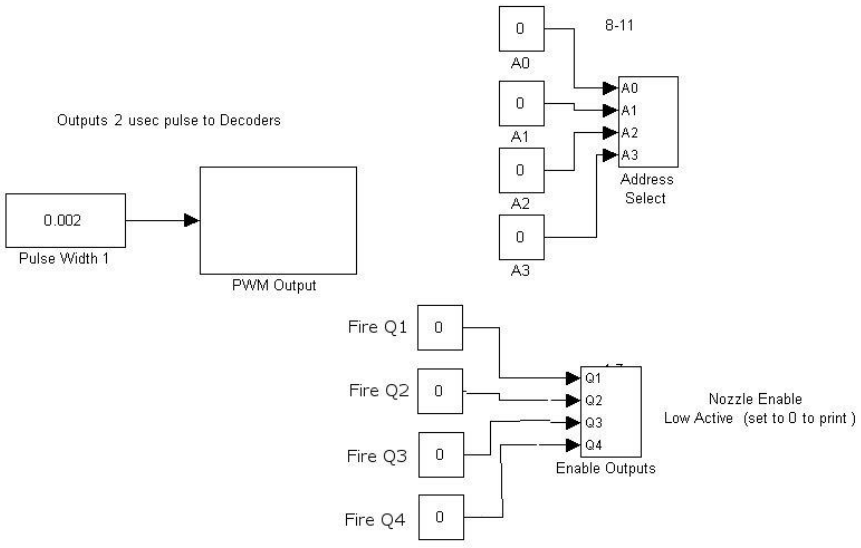

Figure 3-9 Simulink Software to Print with Prototype Board

The outputs from the Simulink software will be delivered to the Driver Board via the digital outputs on the Q8 interface board. The PWM signal will connect to the Driver Board via the CNTR_OUT pin on the interface board.

Breadboard Prototype

A sample single quadrant driver was prototyped on a breadboard. This was used to verify the proposed circuit and as a tool to map the nozzles to the lines on the flex connector outputs of the decoders. Note that there is no way to map nozzles to the cartridge connector, and hence the flex cable, without firing the nozzles. The prototype was verified by using the Simulink software described in the previous subsection to print drops from the selected nozzle. The next step was to map the nozzles to the input address lines to the Driver Board. An x-axis stage LS100-12 (Anaheim Automation, Anaheim, CA) driven with a stepper motor model number 23MD206D (Anaheim Automation, Anaheim, CA) was used to move paper printing media as seen in Figure 3-10.

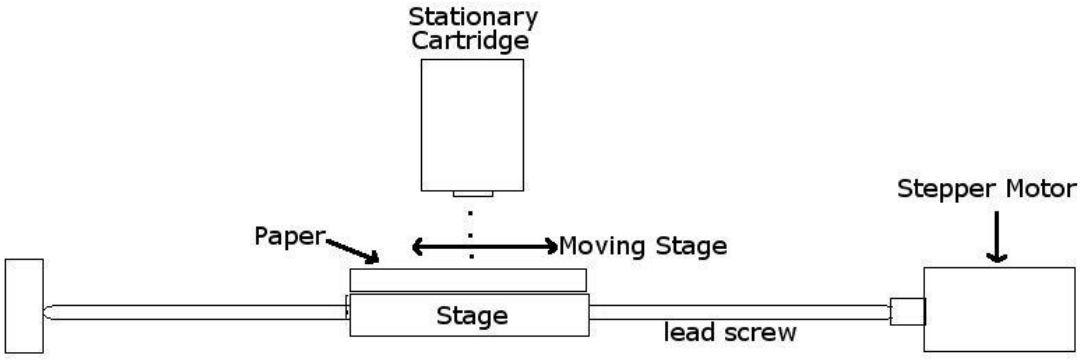

Figure 3-10 Nozzle Mapping Experiment

First the paper was placed under the cartridge and all the nozzles in a quadrant were fired without moving the paper. This created a column of ink dots representing the quadrant that fired them as seen in the left column of Figure 3-11. The stage was then moved 300 microns using an m-file that wrote serial commands to a PCL-601(Anaheim Automation, Anaheim, CA) controller for the stage and the nozzle at the first address (0000) in the quadrant was fired. The stage was moved another 300 microns and the nozzle at the second address (0001) was fired. All nozzles in the quadrant were fired in this manner resulting in Figure 3-11.

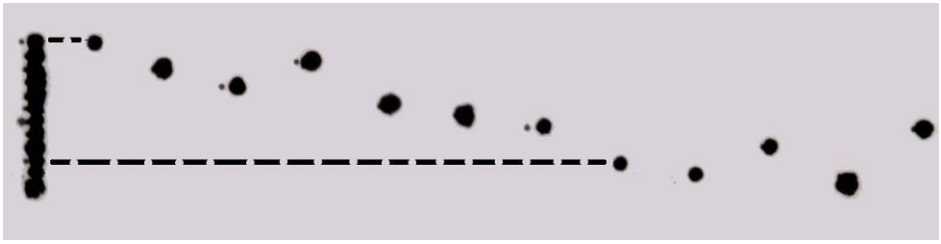

Figure 3-11 Dot Mapping before Correction

Now the relationship between the address lines and dot positions can be established. This was done by matching the order of dots in which they printed, i.e. by sequential address, to their corresponding position in the column. For example, the first dot printed is in the first row of the column print so it is at the correct address (0000). However the eighth dot printed is in the tenth row and so it will be re-mapped to the address (1001). Once this mapping was completed, the corrected mapping was implemented in the test circuit. The result of a test with the corrected nozzle order is shown in Figure 3-12.

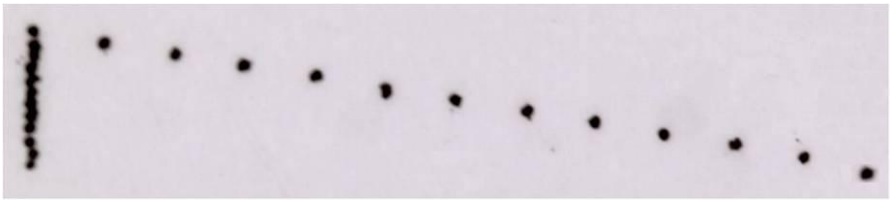

Figure 3-12 Dot Mapping after Correction

PCB Design

After the circuit performance was verified and the order of the nozzles corrected the Driver Board schematic was transferred to the other software in this suite, Ultiboard. Ultiboard provides a PCB layout and design environment with multiple features including auto routing and error checking. The main concerns when placing the traces on the PCB were ground paths and high current paths. This was discovered with the first version of the PCB through the observation of the firing waveform. The waveform had high frequency content at the end of the firing pulse. This was traced to the ground paths providing too much resistance for the high current switching of the transistor array. This information and more accurate information about the size of some of the components were used to create a second version of the Driver Board. To minimize the ground problem a four layer board was developed to replace the two layer board of the first version. The four layer board allowed for a power and ground plane to reduce the effective resistance of these traces. The other two layers were used as signal routing layers to provide more freedom (versus a single layer) in routing the many traces on the 3x4.5 inch board. The resulting layout is presented in the Figure 3-13. The layout shows three of the layers, where the red layer is the ground layer and the white and green layers are the signal routing traces.

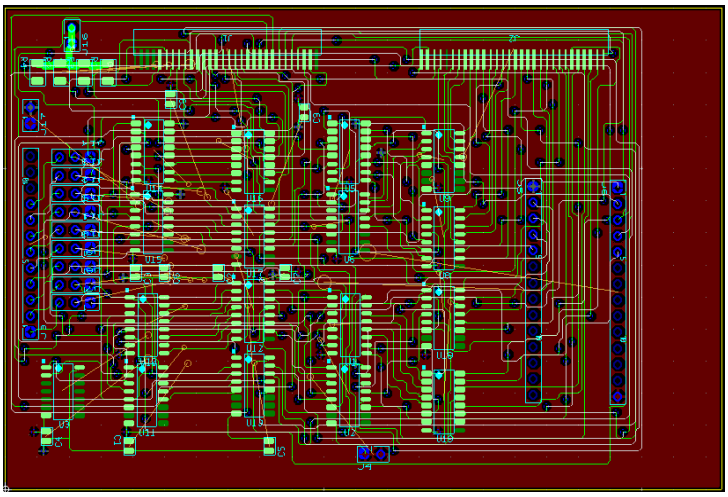

Figure 3-13 PCB Layout of Driver Board

The extra three pin headers and fourteen pin headers were added so that extra functionality can be added through the addition of a daughter card containing a microcontroller. This function would work with the jumpers seen in Figure 3-14 added that allow the input to the Driver Board to be from either the Q8 board or from the headers used to attach the daughter card. This would allow for the microcontroller on the daughter card to control the firing signal from a faster clock speed than the 1 kHz speed of the Q8.

The board was exported as a series of Gerber files, a common format board houses use to construct circuit boards, and was ordered through PCB Express (PCB Express, Mulino, OR). The Driver Board was populated with components using a surface mount soldering station from Zephrytronics (Zephrytronics, Pomona, CA) that included a hot air bath (Airbath ZT-1), an Airmill ZT-5100, and an Airpencil ZT-2. The finished board populated with all its components is presented in Figure 3-14.

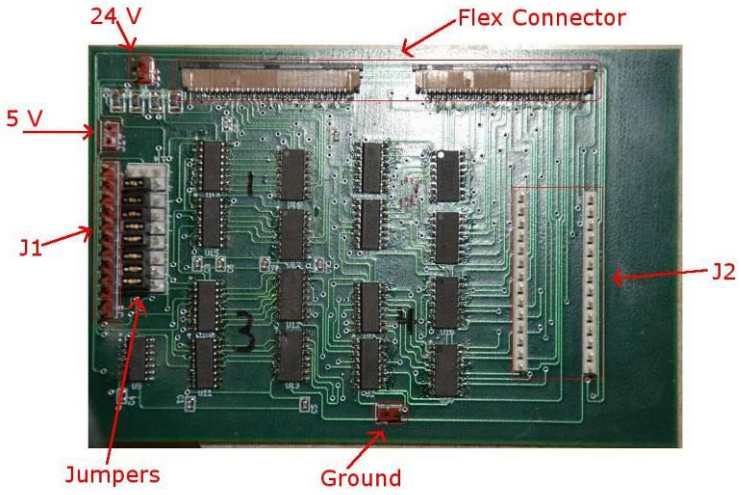

Figure 3-14 Populated Driver Board

After the driver board was built the outputs to the print cartridge were verified. This first was done by connecting a 32 ohm resistor in place of the print cartridge and firing the board as if the resistor was the nozzle we were selecting. During the firing, the voltage drop was measured similarly to when it was measured on the actual HP 520C printer. The resulting waveform was as expected and therefore testing proceeded with the HP26 cartridge in the hardware loop. This was done by firing all the nozzles with the cartridge stationary and counting the number of dots. When this was done, all 50 nozzles had been accounted for, and ink dots were found on the paper used as the printing material.

Cable Interface Board

Different models of the HP 500 series printers use two types of geometric configurations in their flex cables as seen in Figure 3-15.

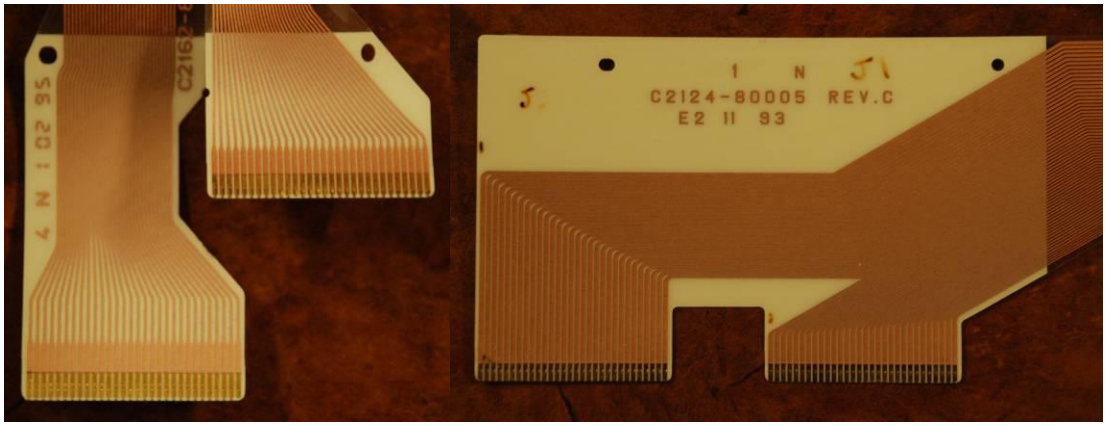

Figure 3-15 The Two Different Types of Flex Cables

The cables have different geometric locations for the contacts, yet the wiring for each connection is exactly the same. The PCB for the HP26 cartridge was designed to accept the second connection. To allow the PCB to use either cable, a simple 2 layer adapter board was designed so that both configurations of flex cables could be used in the system. Circuit Design Suite version 10.0 (National Instruments, Austin, TX) was used again in the design of this adapter board. The connections were a one to one mapping since the only difference in the cables were the geometric locations of the male adapters. This adapter board, shown in Figure 3-16, was necessary to utilize all of the flex cables that had been salvaged from 500 series printers.

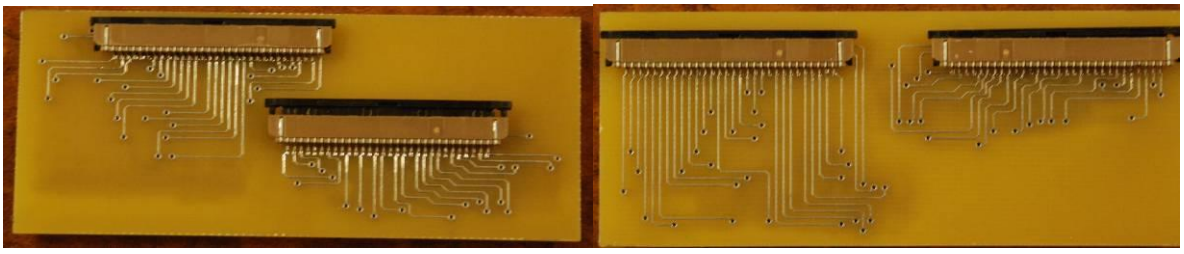

Figure 3-16 Front and Back of Adapter Board

Verification of the Custom Driver Board

The power signal that delivers energy to the printhead was compared to the one observed in the printer. This was done in the same manner as the measurement on the actual printer by using an oscilloscope, model TDS 3034B (Tektronix, Beaverton, OR), to monitor the voltage drop at the node connecting the source resistor to the printhead. The observed waveform is pictured in Figure 3-17.

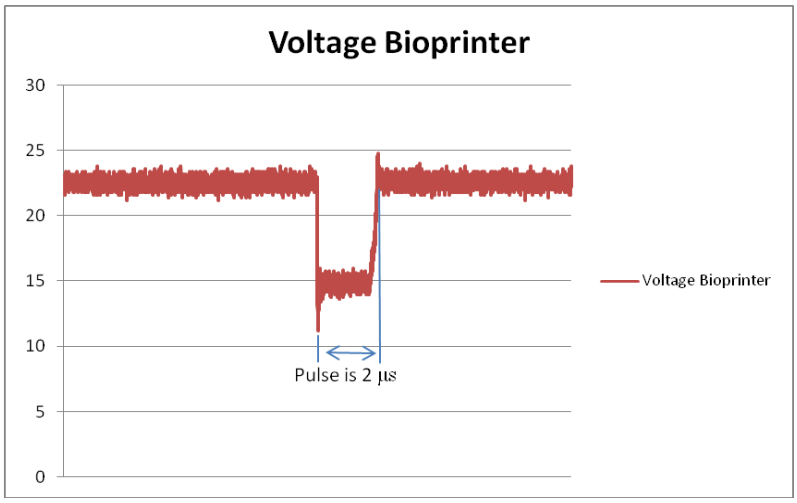

Figure 3-17 Measured Voltage Drop of Custom Driver Board

There is a spike on the falling edge of the waveform and one on the rising edge of the waveform, but the duration of these is less than 50 nanoseconds for each peak, and is most likely a result of the transistor switching in saturation. This waveform is compared to that observed from the actual printer through the difference of the magnitudes of voltages in Figure 3-18.

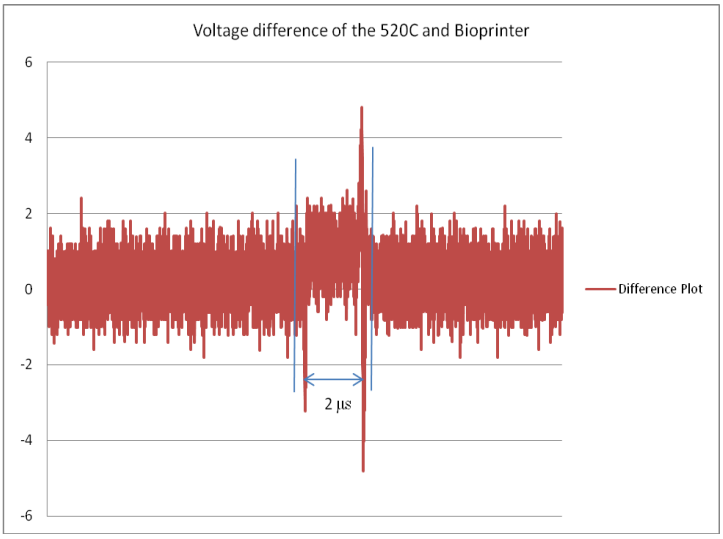

Figure 3-18 Difference of Custom Driver's Voltage Drop and a HP 520C Printer

The figure shows that the waveforms are almost identical, with slightly less voltage being dropped across the printhead thermal resistor in the actual printer shown via the increase in error during the pulse waveform in Figure 3-18. This is due to the source resistor in the actual printer being slightly higher, since the actual value from the printer of 14.7 ohms could not be found and 13.7 ohms was used instead. This increased the voltage drop across the printhead due to the lower divisor in the voltage divider equation however the source voltage could be lowered to match the nozzle voltage. However dot formation and printing do not appear affected by this slight increase in energy or the addition of the high frequency content on the switching of the pulse.

Printing Parameters

The custom design of the driver board allows for once fixed parameters of the 500 series printers to be changed. Specifically, the width of the pulse can now be varied, changing the amount of energy delivered to the nozzles. The effect of this parameter will

eventually be studied on “bio-ink” containing various cells. Another parameter that can be varied in the custom hardware is the amplitude of the voltage across the nozzle. As seen in Equation 3-2 the energy being delivered to the nozzle is directly proportional to the square of the nozzle voltage. The parameter is varied by changing the DC source applied to the power electronics on the board and is determined by the voltage division of the source resistor and the nozzle resistance. Care should be taken when determining these parameters as they can cause failure of the print nozzles due to overheating the nozzle resistor. With the functionality of the driver board confirmed, the effect of varying the firing pulse width and varying the distance from the printhead to the printing surface was studied to determine the optimal printing parameters. These studies were also run to determine the range of possibilities of the cartridge so that they could eventually be run with cells in solution.

Pulse Width

To vary the pulse width for the first study, the duty cycle for the PWM was changed to the desired pulse width. Studies were run with pulse widths of 1.5 to 2.75 microseconds in increments of 250 nanoseconds. A sample of the results that were obtained from the study are presented in Figure 3-19.

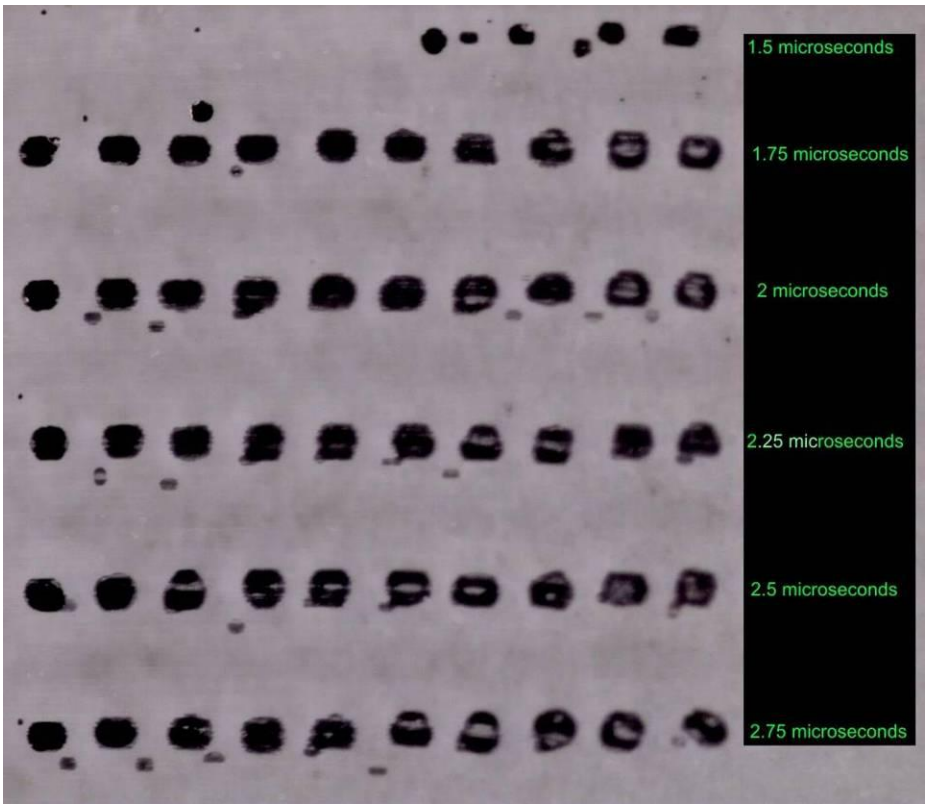

Figure 3-19 Pulse Width Study

The results are roughly the same from 2 to 2.5 μs, however printing for long periods of pulse widths over 2.5 μs causes the nozzle to stop printing without any observation of physical damage. A value of 2.5 μs provides for 15.3 μJoules. Limiting the amount of energy delivered to that value should prevent nozzle damage. The range of pulse widths for acceptable printing was established to be 1.75 μs – 2μs.

Print Height

Now the effect of varying the print height was studied on the formation of the drops on the printing media. This study was run with an adjustable height (z-direction) stage, model LT1 (Thor Labs, Newton, NJ), used to adjust the height of the print cartridge as seen in Figure 3-20.

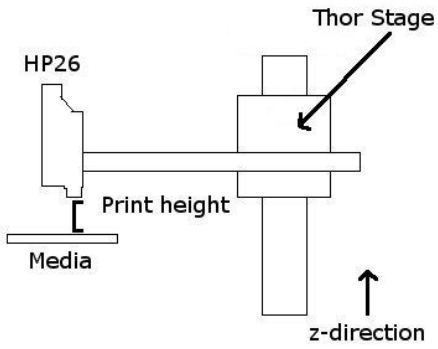

Figure 3-20 Diagram of Print Height Experiment

The height to the print media was varied from 1 mm to 5 mm in 1 mm increments. Samples of the results obtained from this study are shown in Figure 3-21.

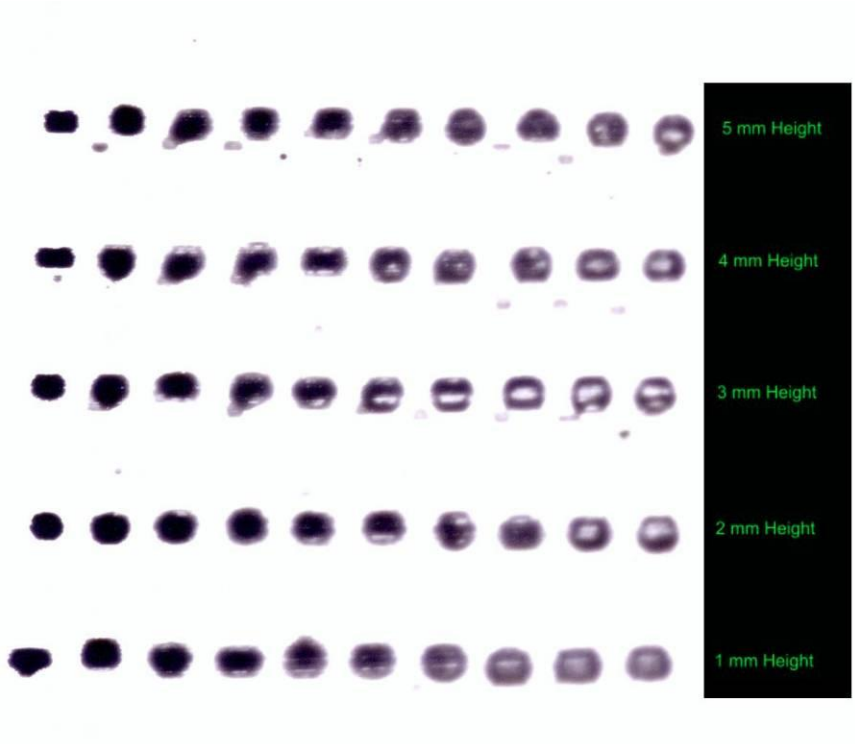

Figure 3-21 Print Height Study

This study was run with the standard observed pulse width from the HP 500 series printer of 2 microseconds. The best results were obtained when the cartridge was 2 mm from the

surface on which the cartridge is printing. Therefore the best parameters to print were determined to be a 2 microsecond pulse with the cartridge being at a height of 2 mm from the surface.

Conclusions

The custom driver board developed in this section reproduces the nozzle firing capability of the drive electronics of the HP 500 series printers. The waveforms generated match the firing waveforms of the original printer and accurately fire all of the nozzles. The custom hardware also allows for variable parameters on the firing waveform to study the effect on drop formation and printing. One aspect not implemented in the custom driver board is the monitoring of the saturation voltage of the BJT transistor. Adjusting the pulse width in response to saturation voltage was judged to be a second order effect that would have relatively minor effect on printing, especially at the reduced printing speed of the current system. The driver board was an overall success and allows for total control of the HP26 cartridge.

CHAPTER FOUR
DESIGN OF A TWO DEGREE-OF-FREEDOM SINGLE CARTRIDGE BIOPRINTER

The Bioprinter was built by integrating the Cartridge Driver, described in Chapter 3, with a 2-axis positioning system, and a PC with MATLAB/Simulink (Mathworks Inc, Natick, MA) and Wincon (Quanser, Ontario, Canada) to produce a two-dimensional (2D) ink-jet printing system. Two primary concerns in the design of the bioprinter are accuracy of dot placement and the capability to swap out the cartridges and accurately print from the second cartridge after swapping. These driving factors were addressed in the design of the single cartridge bioprinter which accepts a bitmap image as input to be printed.

Design Overview of the 2-D Bioprinter

Design Specifications

Before the design of the 2-D Bioprinter began, a list of design specifications was generated so that the printer would function as needed and choices could be made to select components during the design. The major design specification for the Bioprinter was the accuracy of the placement of the ejected dots on the media. The goal of 50 micron accuracy along each axis for axis positioning was estimated to be adequate considering the size of the drop (160 microns) and the unknown repeatability of depositing drops with the HP26 cartridge as depicted in Figure 4-1. Another design specification considered during the design of the Bioprinter was to allow for variable print resolutions from the inherited resolution of the HP26 cartridge of 86 microns and greater.

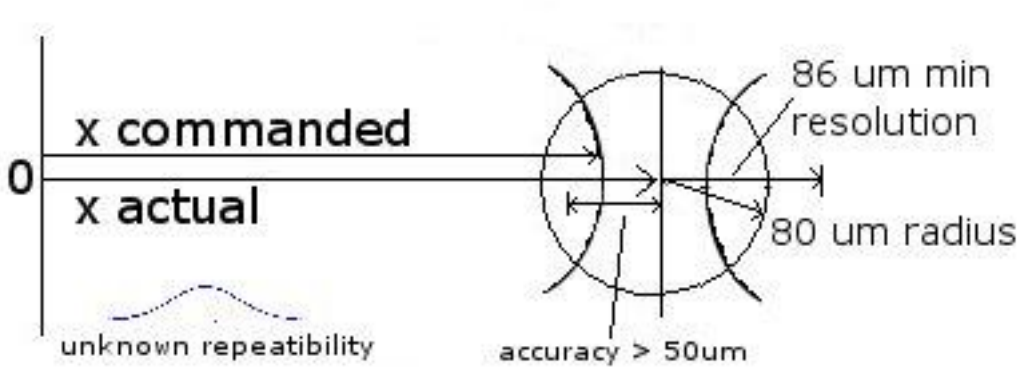

Figure 4-1 Printed Drop Accuracy

The ability to swap cartridges on the fly and print with different cartridges accurately was another design specification along with size (needed to fit in cell hood), the ability to be sterilized, and ease of operation by a trained technician.

Overview of Proposed System

The proposed system contains a 2-D positioning system that moves the print media, while leaving the print cartridge in a single position. The decision to move the print media instead of the print cartridge, unlike the traditional ink-jet systems was based i) upon the ease of designing a sample holder that moved with the 2-D positioning system ii) difficulty of designing cabling to move with the electronics that control the print cartridge and iii) the flexibility of adding other fixed stations, such as a microscope, to analyze or manipulate the samples. In Figure 4-2 a block diagram of the overall system is presented with the major components of the Bioprinter.

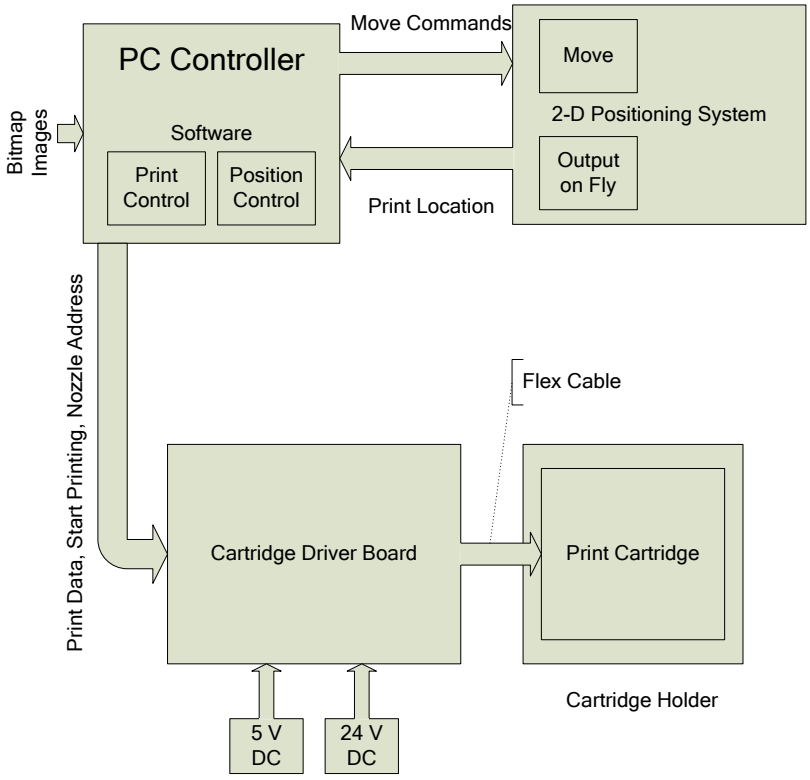

Figure 4-2 Overall Block Diagram of Bioprinter

The design of the Cartridge Driver Board and the connection to the carriage holder and cartridge were described in Chapter 2. The PC controller hardware was also discussed in Chapter 2 and only new software will be required to control the printing system and integrate the components. The major design task is the 2D positioning system.

2D Positioning Stage

The weight that the stage had to move was not a concern since the loads applied to carry the stage and multiple slides is not a limiting factor with systems that are commercially available. The limiting design specification for selecting the stages was accuracy and repeatability. The stages were chosen based upon their accuracy and affordability, along with their ability to easily add another axis to provide a 3-D system in

the future. The 2D positioning system was constructed using linear positioning units from Anaheim Automation (Anaheim Automation, Anaheim, CA). Several options were considered before choosing the solution from Anaheim Automation (http://www.anaheimautomation.com). In Table 4-1 the alternative choices are listed. The stages from Anaheim Automation were chosen due to their linear screw design, cost, and accuracy.

Arrick Robotics (Tyler, TX)	Belt drive Parallel port Accuracy +/-.010" per foot MD2xp interactive motion control program	Table XY-9 9"x9" = $750.00 US Z axis = $400 MD2xp = $1,000.00 ~ total = $2,500
Griffin Motion (Holly Springs, NC)	This stage utilizes a preloaded lead screw with integrated stepper motor. 2 micron repeatability is attainable in the Travel Range of 50mm X 50mm to 200mm X 200mm Servo or stepper motors interface communication utilizes RS232, however, RS422 and USB are also available. This controller can be programmed for stand alone operation. Z available	Complete 3 axis system ~$20,000
Conix Research (Springfield, OR)	X, Y axis travel - 7.9"x 4.3" X, Y axis Repeatability 25um X, Y axis Resolution 0.7um Z axis Resolution - 1um Z axis travel - 35mm Tabletop unit size is 16.25"D x 17.25"W x 14.5"H Total weight - 23.5 lb	**Retail Price $6175.00** System includes: Motorized XY-Stage, Z-Module, and Controller.
Anaheim Automation (Anaheim, CA)	X, XY, and XZ Stages Up To 25 lbs. Load 6", 12", and 18" Travel Options Low Profile 3.5" x 3.5" Carriage Resolution Options from .000156" to .001250" Precision Rolled Acme Screws	

Table 4-1 Options for 2D Positioning Systems

The x-axis is a LS100-12 (12” travel) coupled with a stepper motor from Anaheim Automation model number 23MD206D and the y-axis is a LS100-6 (6” travel) with the same stepper motor. The stepper motors were equipped with a 1000 count encoder from US Digital (US Digital, Vancouver, WA). The stages themselves are lead-screw linear stages, which advance 1/16 inch per revolution of the lead-screw. The error in position for one stage is 250 microns per every meter traveled thus providing an error of 0.39 microns per revolution of the lead screw.

Motion of the linear stages is controlled by another Anaheim Automation product, the PCL601 Programmable Step Motor Controller. The controller allows for the stepper motor to operate in full step, 1/2 stepping, 1/4 stepping, and 1/8 stepping modes. The finest resolution is obtained when the 1/8 stepping is employed; however, this reduces the maximum speed at which the motors can operate. This controller allowed for serial communication (RS485) with a PC and also had a feature for position based output called output-on-the-fly. This feature outputs a pulse when the stage is at a specified location. The pulse can be used to synchronize print commands with motion commands.

Each axis requires a 24VDC 65 Watt supply. Three 24 volt DC power supplies were bought and built into a box that had a cooling fan and toggle switches to turn the individual supplies on and off. A power supply was needed to power each of the axes while the third was used to produce a 5V DC through an evaluation board from National Semiconductors, part number C2006, which acts as a DC-DC converter. This 5V supply is used to power the output-on-the-fly feature from the PCL601 which is an open collector output that is pulled to 5V through a 1 kΩ pull-up resistor. These supplies were

also bought from Anaheim Automation and were part number PSAM24V2.7A. The entire power setup for automation is pictured in Figure 4-3.

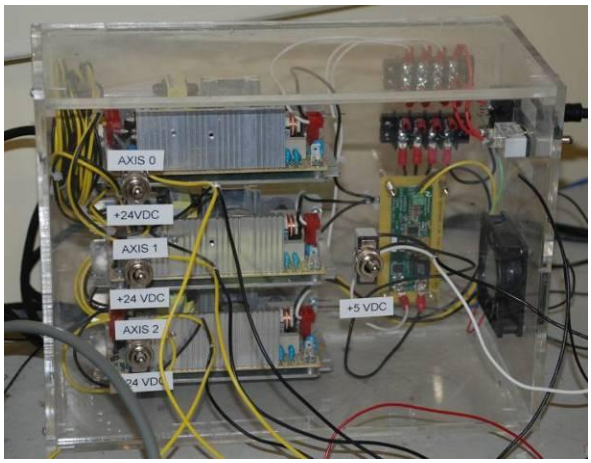

Figure 4-3 Power Supply for Stage

A top view of the assembled mechanical components is shown in Figure 4-4. The current position of the stage at the bottom right of Figure 4-4 is the origin of the stage coordinate system. In the picture, movement to the left corresponds to the negative x-axis and movement up corresponds to the positive y-axis. This stage moves the print substrate, while the printhead remains at a constant location.

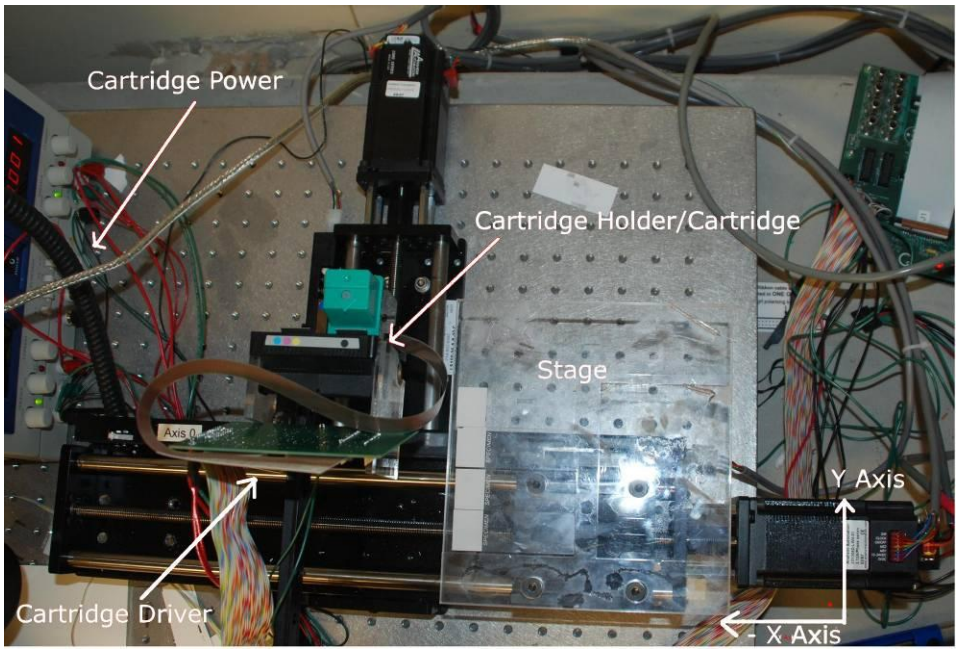

Figure 4-4 Bioprinter 2D Stage

The stage, seen in Figure 4-4, is an acrylic base made of three layers and built to hold ten slides. The dimensions of the stage, 7”x7 ½“, were chosen to be able to hold ten 3”x1” slides. To accomplish this with a 6” vertical axis, the slides need to be arranged in two columns. The stage could be expanded to include another column of slides if needed, thanks to the 12” range of the x-axis. The acrylic stage was drawn using AutoCAD 2007 (Autodesk, San Rafael, CA) and then cut from an acrylic sheet 6 mm thick using a VersaLaser 200 laser cutting machine (Universal Laser Systems, Scottsdale, AZ). The bottom two layers of 6 mm acrylic provide a flat base as seen in Figure 4-5. The third layer of 3 mm thick acrylic provides the structure for holding the slides. Metal strips were used to apply force to push the slides stacked next to each other against the supporting structure and thus hold slides in place by friction. The top slide on the right column is used for the alignment pattern discussed later in this Chapter. The stage was attached to

the positioning system via four bolts. The detailed layout of the stage can be seen in Figure 4-5.

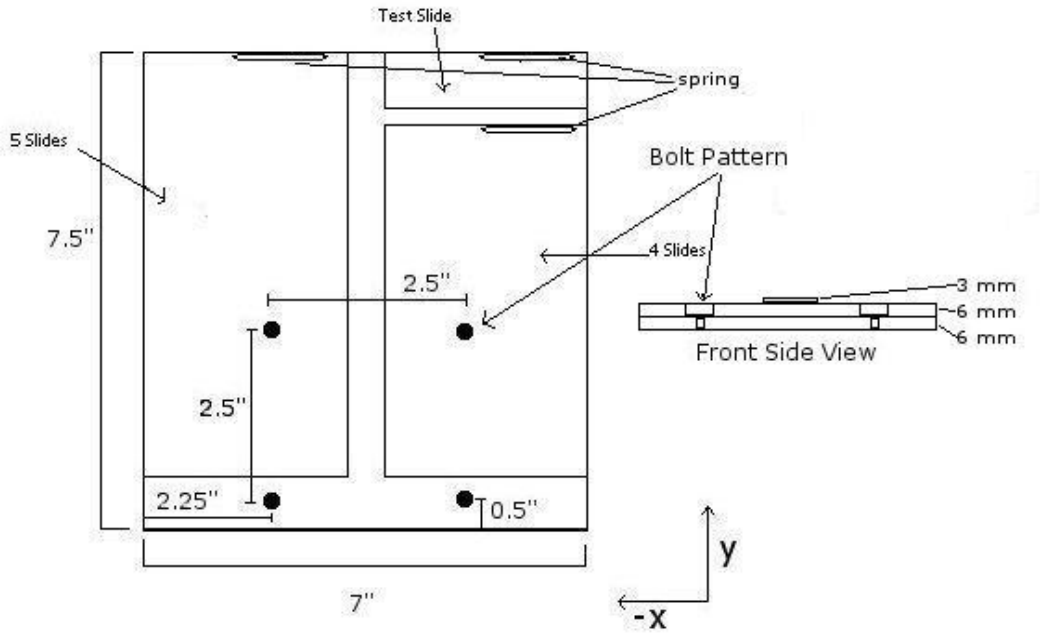

Figure 4-5 Stage Layout and Dimensions

The cartridge holder is salvaged from the carriage assembly of a HP 500 printer. The carriage mount in the system was constructed to support the carriage relative to the moving stage and is built from manufactured parts of acrylic and purchased parts from Thor labs. The full assembly is pictured in Figure 4-6.

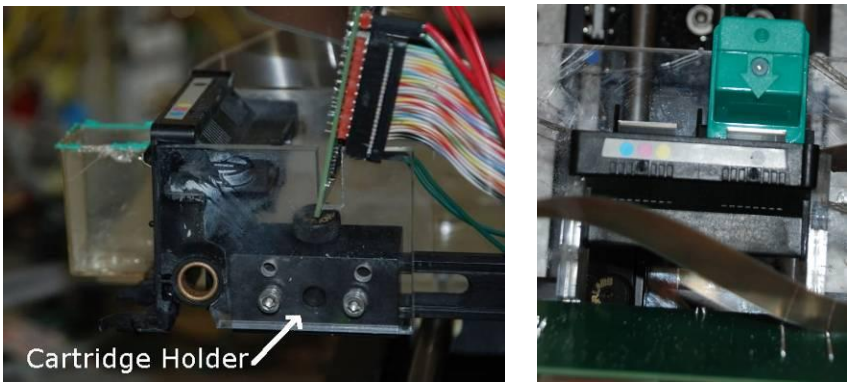

Figure 4-6 HP 500 Cartridge Holder Assembly

The cartridge holder assembly was attached to a two inch, single-axis manual translation stage from Thor Labs (Thor Labs, Newton, NJ), part number LT1, via a twelve inch dovetail rail from Thor Labs, part number RLA1200. The manual stage permits the distance from printhead to print substrate to be adjusted. The dovetail rail was then attached to the carriage via a holder constructed of 6 mm thick acrylic which can be seen in Figure 4-7.

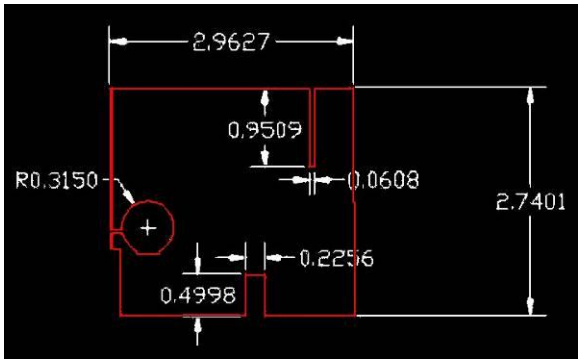

Figure 4-7 Carriage Mount

The holder was made with an identical piece on both sides of the carriage, and the slot in the top of Figure 4-6 holds the cartridge driver board. This setup was then attached to an isolated 2'x3' mechanical breadboard from Thor Labs, part number PBI11106, via a 1.5" diameter steel post from Thor Labs (P6A) and is shown in Figure 4-8.

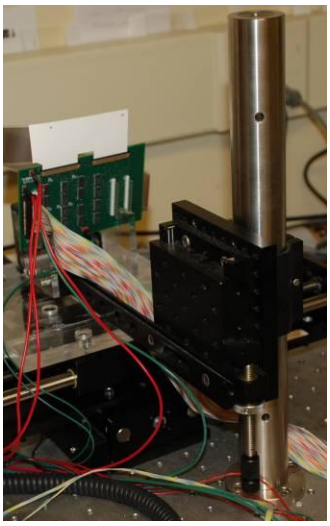

Figure 4-8 P6A Steel 1.5" Diameter Post

Software Design

Software Overview

The software used to print with the custom system hardware consists of several functions that run real-time Simulink models in Wincon and as MATLAB functions in normal Windows XP (Microsoft Corp, Redmond, WA). The software loads the image in a bitmap format (color or b/w) and converts it to a matrix of ones and zeros (black=1, white=0) that has the dimensions of the image. The real-time software component is responsible for transmitting the data to the cartridge driver board and for providing timing to fire the nozzles.

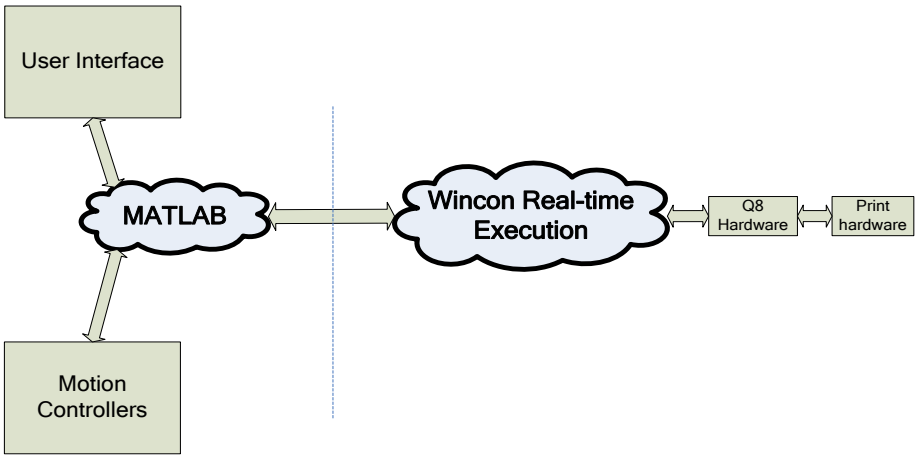

Figure 4-9 Real-Time Interface to PC

The MATLAB software is responsible for moving the stage and provides the user interface. The major facets of the software can be seen in the flow chart in Figure 4-10.

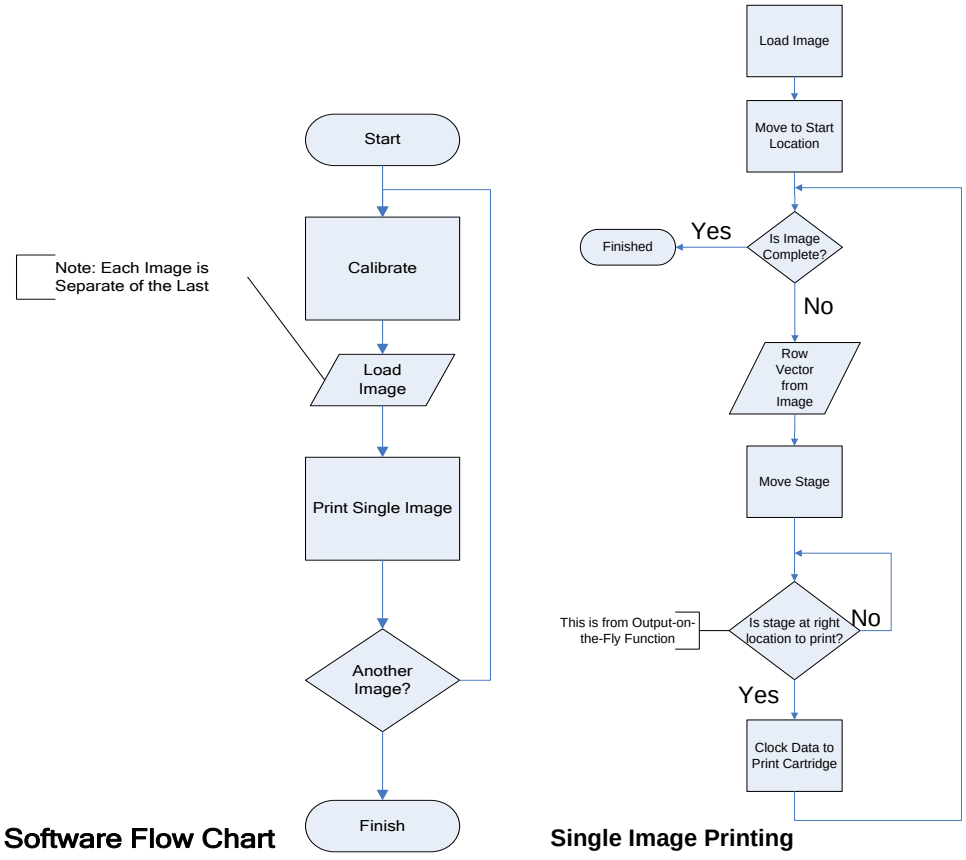

Figure 4-10 Software Flow Chart Image Printing

The software as seen in Figure 4-9 was broken into two applications running simultaneously that transfer data back and forth. MATLAB was used to handle all the communication with the controllers through Simulink and m-files. A Q8 data acquisition card from Quanser provides real-time data transmission to the Bioprinting system and is controlled through integrated Simulink blocks. A functional decomposition of the software is presented in Figure 4-11.

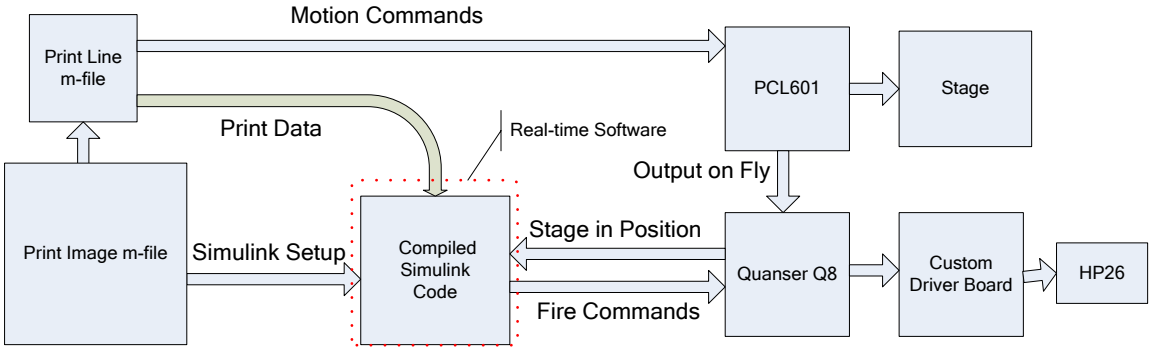

Figure 4-11 Functional Decomposition of Software

Simulink Software

The Cartridge Control program is responsible for receiving timing information from the PCL601 controllers, as well as transmitting the image data to be printed to the driver board via the Quanser Q8. The program is written entirely in Simulink and is controlled through the main print program in MATLAB. It serves as the communication front end to the driver board, transmitting all the required signals to print. Figure 4-12 shows the Simulink diagram used to operate the driver board.

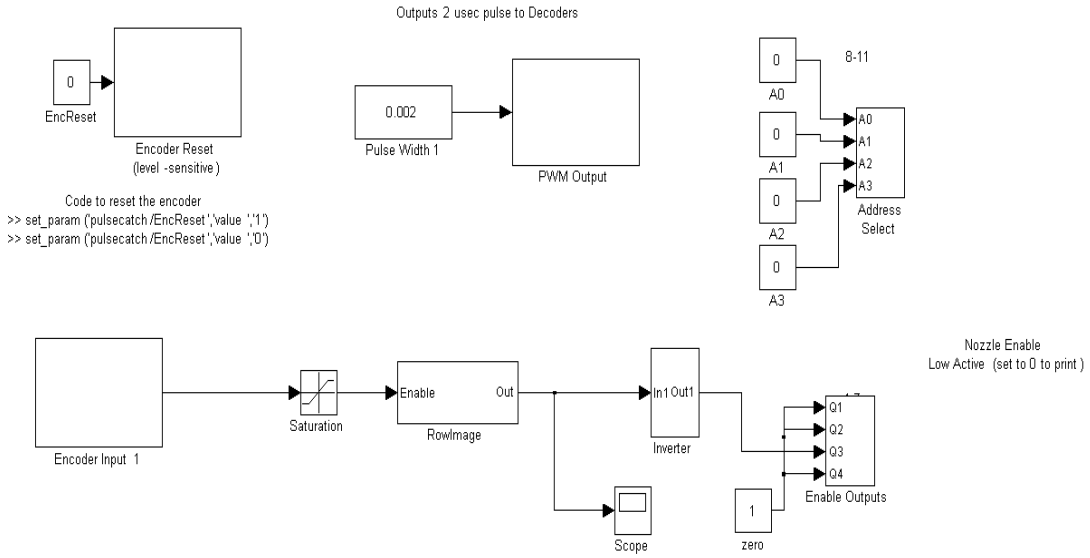

Figure 4-12 Simulink Real Time Diagram

The functionality of the Simulink software can be described in the block diagram above that is compiled into a real-time program. The PCL601 controller inputs a 50 microsecond pulse (output-on-the-fly) to the encoder input of the Q8 board to initialize printing when the x-axis is at the proper location and velocity. The encoder input is used due to the Q8 using a faster clock speed of 2 MHz to update the register which allows for more accurate detection of the 50 microsecond pulse. Since the encoder input is an incremental counter and is incremented in a register on every quadrature pulse it receives, there needs to be a reset of the register storing the current count so that the encoder register will be reset to zero, thus disabling the real-time software until the next row is ready to print. This is done after each line of printing by setting the EncReset constant block to one and then back to zero. When the encoder input receives the pulse from the PCL601 controller, this enables the RowImage block of the Simulink software. Inside this Simulink block an s-function was custom built as a bit-shift register to clock out bits

of the image passed from the m-file and is representative of the “Clock Data to Print Cartridge Block” in Figure 4-10 and a block diagram is presented in Figure 4-13.

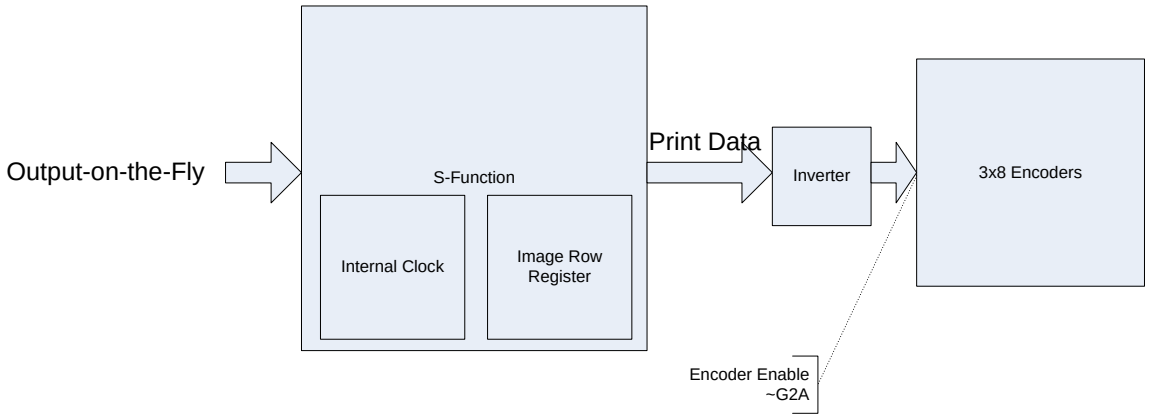

Figure 4-13 "Clock Data to Print Cartridge" Block Diagram

The s-function is enabled from the output-on-the-fly signal and stores the current row of the image printing. It has an internal clock that is used to clock the data out at a user defined period that is a multiple of 1 kHz. Since this output is a one every time a drop is fired and the enable of the encoders of the quadrant firing are low active, there is an inverter block inserted into the output line. In Figure 4-14 a timing diagram is presented that shows when events occur during the operation of the software.

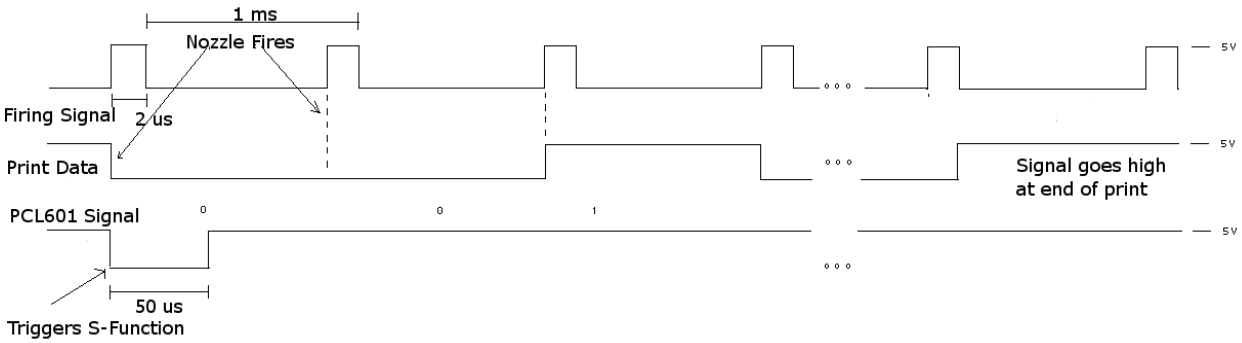

Figure 4-14 Timing Diagram of Printing Software

The address blocks simply output the selected nozzle in the quadrant via the digital outputs on the Q8 board to all encoders. The values are set inside the m-files printing the desired image. The PWM block outputs the high active enable for the encoders as a customizable pulse that is created via the 1 kHz clock speed that the Quanser Q8 board operates. This limits the speed of printing a single dot to 1000 dots/s. The duty cycle parameter of the block is accepted as an input and is set via the m-file.

The s-function is the most important aspect of the Simulink software. If the timing of the internal clock is off slightly the accuracy of the dots is affected greatly. The s-function takes three parameters, the row of the image that is being printed, the length of the row, and the period of the clock speed at which dots are being printed. The s-function updates an internal counter, ct, with another counter, ct2, that increments every clock tick when the modulus of ct2 and the period equals zero. The s-function also ensures that the output of the block is always zero if the counter is greater than the length of the vector to be printed.

M-File Software

Single Cartridge Printing

The m-files constituting the interface and motion software for the Bioprinter act as the main level of software that initialize and operate the flow of the entire system. The main purposes of these scripts are to: 1) Establish serial communication with the PCL601 controllers 2) Determine speed and acceleration profiles for printing 3) Process the input and pass to Simulink 4) Set the parameters for the driver board. The m-files are the main

level of software that brings the individual components from the stage and from the driver hardware into a single, usable system.

The velocity at which the motors can operate is a limitation that results from the physical construction of the stepper motors. The maximum velocity is also dependent upon the type of stepping used to drive the motors. The values were determined empirically for 1/8 stepping, since this is the mode used to drive the 2D stage. This value is 10,000 micro steps per second for 1/8 stepping. Similarly the stepper motors have a maximum acceleration limit of 5000 steps/s^2. This limitation was determined experimentally for the mechanical setup. These limitations were used along with the equations used to ascertain the speed and acceleration distance to develop rules of thumb when setting the parameters for printing. In order to print a dot every period ms at a distance $pixelspacing_x$ μm apart, the stage velocity should be

$$v = \frac{pixelspacing_x}{period} \qquad (4.1).$$

Period must be an integer multiple of 1 ms, which is the sample period for the WinCon system. The width of the printed image is

$$Printwidth = image_{width}\, pixelspacing_x \qquad (4.2),$$

where $image_{width}$ is in pixels. To ensure that the x-axis of the 2D stage is at constant velocity before reaching the point to start printing, a distance is calculated using the velocity and acceleration. This distance is the acceleration distance needed for the given velocity for the axis to reach constant speed. From calculus,

$$d_{\text{acc}} = \frac{v^2}{a} \quad (4.3),$$

where a is the acceleration and v is the final velocity. Given these parameters the software can accurately tell the PCL601 controllers what position of the stage to pulse the output on the fly function.

Reaching constant velocity is a major aspect in obtaining repeatable, accurate prints. The ability to determine the exact location to print the line when constant velocity has been reached has already been shown. The need for constant velocity arises from the open loop nature of the printing. Since there is no state feedback every timed occurrence must be synced to the 1 kHz clock that is provided through the Q8 board. This means that if the velocity changes or is not constant at the beginning of the print then the bitmap coordinates will not be in the same location line to line as seen in Figure 4-15.

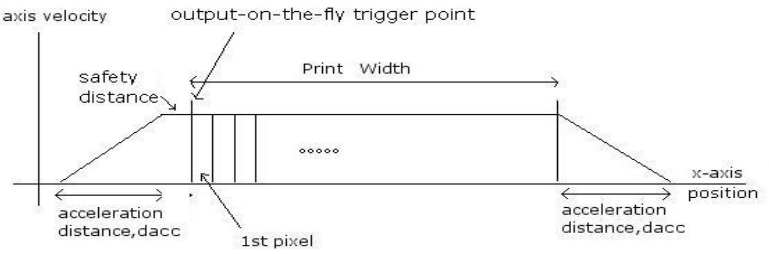

Figure 4-15 Axis Velocity Profile

Therefore the necessity of obtaining the steady state velocity is imperative.

The m-file software uses MATLAB's image processing capabilities to load an image into memory and manipulate the image into a binary matrix. The built in functions

of imread and im2bw are used for these purposes. Once the image is loaded into memory and converted to a binary matrix the stage is sent to the proper location to begin printing through commands to the PCL601 controller. Once the stage is in the proper location, i.e. the upper left corner of the image, the first row of the image is passed to the s-function described earlier. Then the output on the fly is set depending on whether the stage is moving left-right or right-left. Next the x-axis moves the proper distance, taking into account acceleration distances on both ends of the movement. When the stage reaches the initial location plus or minus the acceleration distance depending on the direction of travel, the PCL601 controller outputs a 5 volt pulse to the input of the encoder channel on the Q8 board. This triggers the s-function to start clocking out the row of the image using the 1 kHz clock subdivided by the period to ensure proper firing speed with stage movement. The print program only uses one nozzle from the cartridge to print the line from the image. Once the row is completed the y stage moves the y-distance spacing and the software waits for the PCL601 controller to return a not busy signal on the serial port and then the operation is done again.

Two Cartridge Calibration

When a cartridge is removed and replaced or a second cartridge is installed, there can be a change in position of the nozzles of the second installation relative to the first as depicted in Figure 4-16.

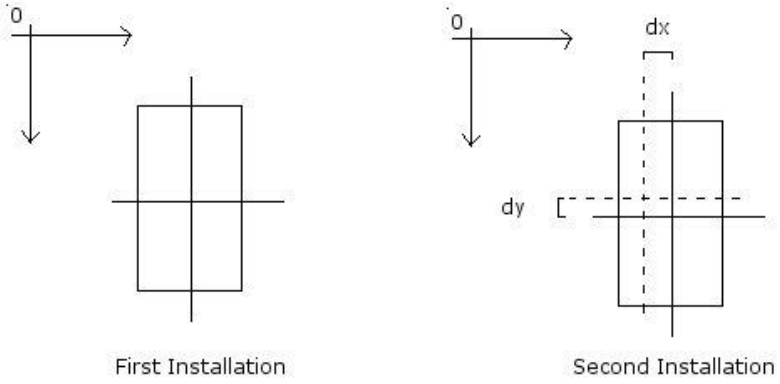

Figure 4-16 Nozzle Offset Between Cartridges

This is not an issue when only one cartridge is used, however multiple cartridges are desirable since this will allow multiple materials to be printed with repeatable, accurate results. A calibration is required; that is, the 2D difference in position from mechanical movement during the replacement of the cartridges (dx and dx in Figure 4-16) needs to be estimated and integrated into the motion of the second installation. The calibration problem is solved using a retrograde Vernier scale where the first cartridge installation prints the "data" scale and the second cartridge installation prints the "indicating" scale. This algorithm works by attempting to form a discrete approximation to the offset caused by the change in position when switching print cartridges. Three potential cases arise when examining the scales - first the "indicating" scale's first line can be higher than the first line of the "data" scale, secondly the first line of both scales can be at the same location, and thirdly the first line of the "indicating" scale can be lower than that of the "data scale". An algorithm will be developed to address these cases and quantify the amount of shift. These cases are demonstrated in Figure 4-17.

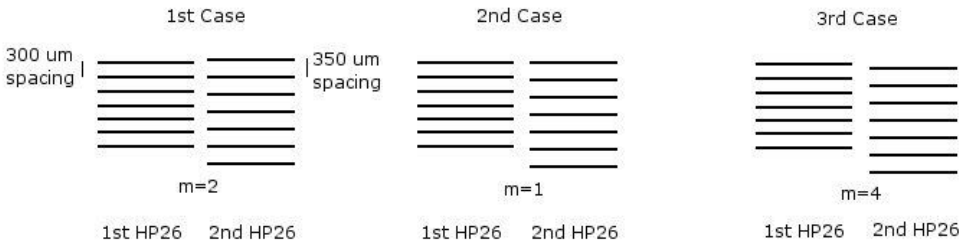

Figure 4-17 Calibration Examples

To this end, a set of n+1=7 horizontal lines is printed at a distance of 300 microns from each other on the y-axis to create the "data" scale. These lines will be used to estimate the error induced in the y direction from changing the print cartridge. To account for the error in the x direction a group of 7 vertical lines will also be printed a distance of 300 microns apart as the data scale. Both groups of lines together form the first half of the calibration routine as shown by the pink colored lines in Figure 4-18.

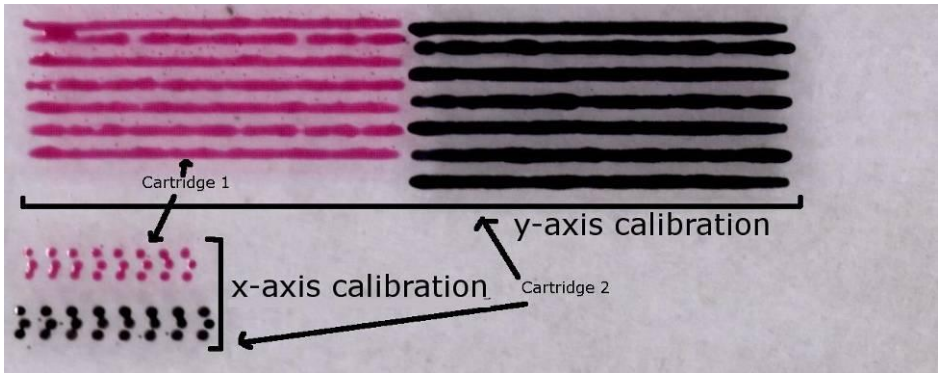

Figure 4-18 X and Y Calibration Pattern

The second half of the scale, the "indicating" scale is now printed. The n lines in the "indicating" pattern are printed 300μm/n = 50 microns farther apart from the distance the first pattern, i.e. 350μm line spacing, was printed. The variable m is assigned to be the line number of the "indicating" print that best matches a corresponding line in the "data" print. If m=1 no offset is required since the offset is then less than 50 microns. If the first

line of the second test pattern appears higher than the first line of the first pattern then the offset is

$$offset = \frac{(m-1)*300\mu m}{n}. \qquad (4.4)$$

If the first line of the second test pattern is lower than the first line of the original pattern then the offset is

$$offset = -\frac{(n-m+1)*300\mu m}{n}. \qquad (4.5)$$

The accuracy of this calibration will be 300μm/n = 50 microns. The offsets are then used in the motion control to create constant motion offsets of the second cartridge installation relative to the first.

To complete the calibration example in Figure 4-18 the cartridges are switched, after having printed the relevant calibration image with the first cartridge, and the second pattern, the one in black in Figure 4-18, is printed. When it prints the second pattern the first line is printed assuming no error was introduced to the system. In this example the "scale" image is shifted down from the "data" image and the second to last row of the "scale" image best aligns to the "data" image. This results in m=6 for equation 4.5 to estimate an offset of 50 microns in the –y direction. Similarly, m=4 will be used in equation 4.4 to estimate an offset of 150 microns in the positive x direction. The results of the calibration routine are shown in Figure 4-19 where two different color inks have been printed after the calibration procedure. The large spots are the printed dots while the

smaller dots are an artifact of the printing process discussed in the "Verification of the Overall Bioprinter" section below.

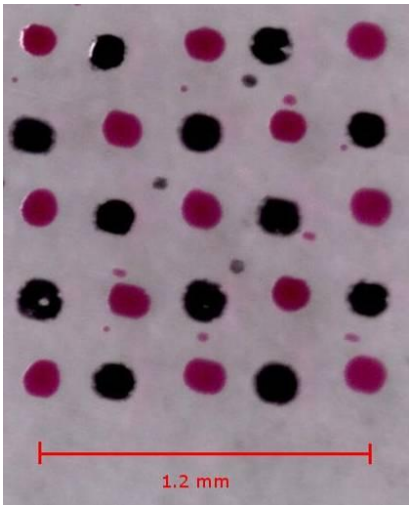

Figure 4-19 Checkerboard Pattern after Calibration Routine

Each dot in the print is approximately 300 microns from the other dots in both the x and y direction. This algorithm along with the Bioprinter setup allows for multiple cell types to be printed at the single drop resolution with accuracy up to 50 microns that will be shown in the next section. This approach assumes that the nozzle columns are co-linear – i.e. no rotation between cartridges. A camera system could be utilized to obtain accurate calibration between cartridges by calculating the offset on the fly. The approach requires an additional calibration pattern for each additional change of the cartridge.

Verification of the Overall Bioprinter

Limitations of Inkjet Printing

During printing with the HP 500 series of printers and with the Bioprinting system several satellite drops have been observed as seen in Figure 4-19. These can be

the result of two phenomena: the formation of a smaller drop that breaks away from the main drop when printing or the formation of a smaller drop as the main drop hits the media and breaks away. These hypotheses can be seen in Figure 4-20.

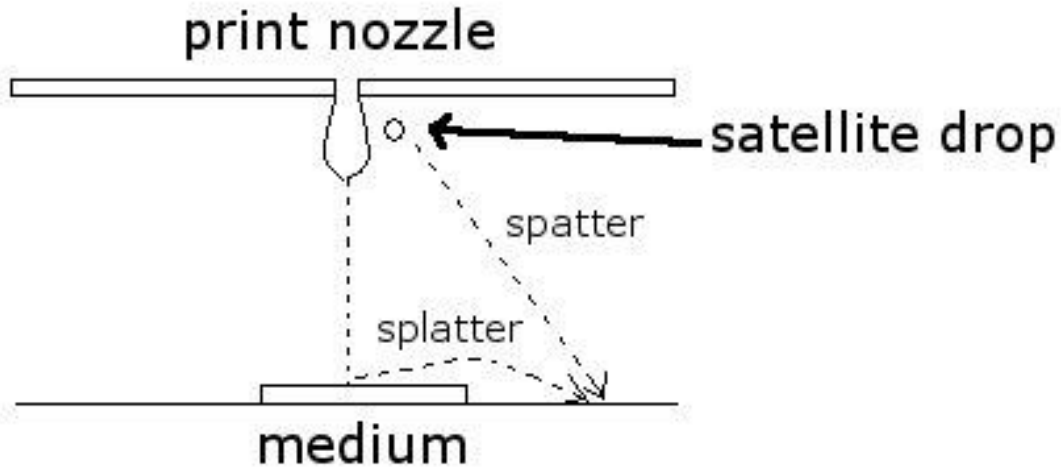

Figure 4-20 The Definition of Splatter and Spatter

The closer the printhead is to the media in either system the lesser the amount of satellite drops noticeable. The satellite dots seen in the image are splatter from the drops and are reduced when the printhead is lowered to the proper height of 2 mm to the print surface. Piezoelectric printers can produce complex firing waveforms that have been shown to reduce the number of satellites [13]. The thermal inkjet's inability to handle satellite drops in this manner could prove to be a potential weakness.

This phenomenon was also observable in the HP 520C printer as seen in Figure 4-21. There is clear formation of satellite drops outside the intended print pattern at the height designed into the printer. This leads to the hypothesis that the satellite drop is a result of the print cartridge not the custom Cartridge Driver Board.

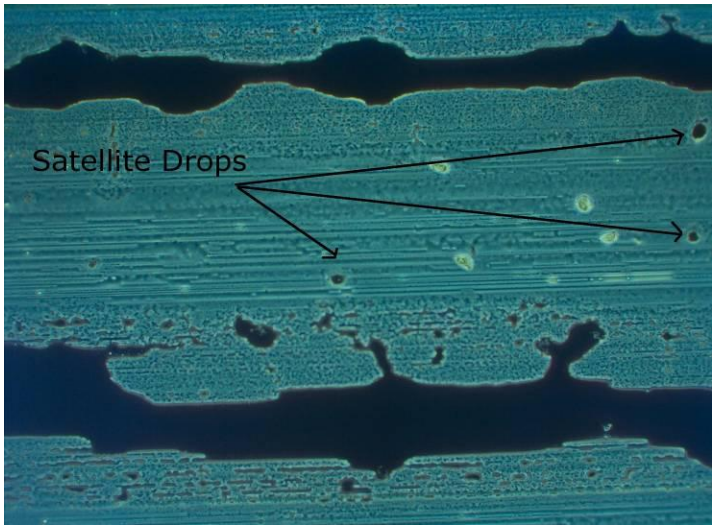

Figure 4-21 Satellite Drops from the HP 520C

Demonstration with Ink

With the custom driver board integrated into the 2D stage and software written to control both, the capabilities of the Bioprinter were determined. As proof of concept, several different patterns were selected as test images - among these were photo quality prints, artificial patterns, and geometric shapes. The printer was also tested with several cell types with simple test patterns. The following figures are some of the results that show the ability of the system to print large-scale images.

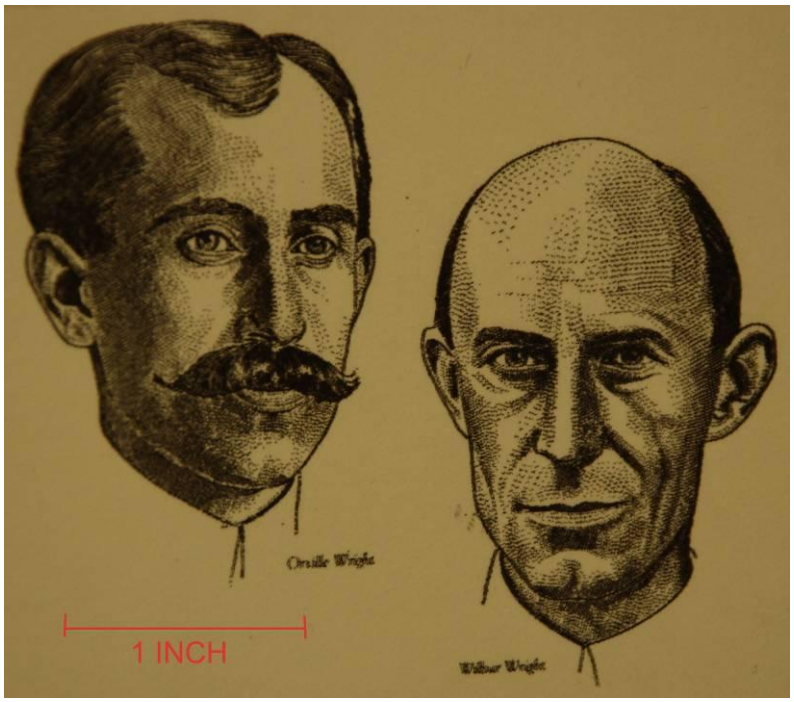

Figure 4-22 Picture of Wright Brothers Printed on Bioprinter in Ink

Figure 4-23 Tigerpaw Printed on Bioprinter in Ink

Figure 4-22 and Figure 4-23 demonstrate the capability of the Bioprinter to print large complex patterns. These images are printed with black ink.

The ability to accurately print patterns at the resolution of the drop size of the HP26 cartridge was the ultimate goal in building the Bioprinter. This will provide the means to accurately pattern different types of cells and study their interaction with one another. Figure 4-24 illustrates the ability to print on a smaller scale.

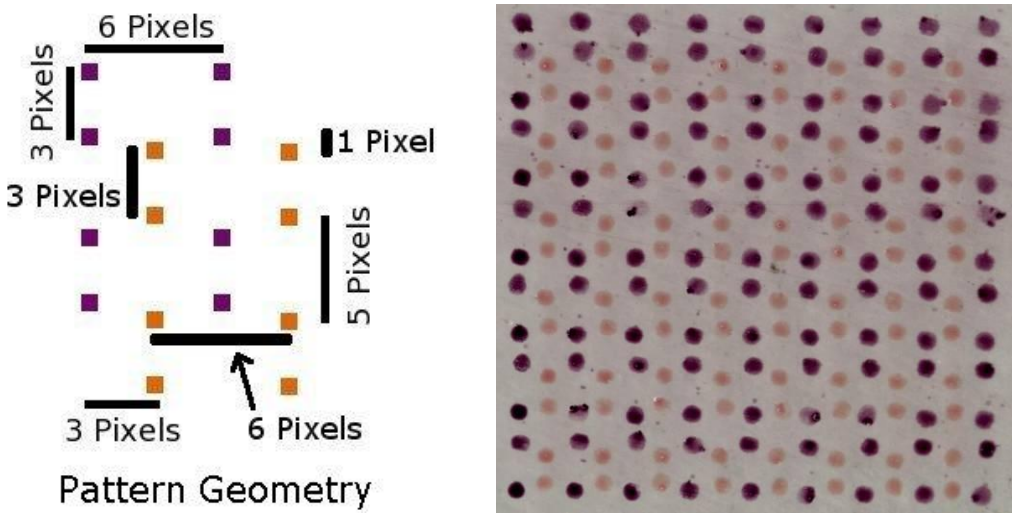

Figure 4-24 Single Dot Pattern a)No Error Pattern b)Printed Pattern at 1.25x

To determine the relative accuracy of the printer, the x and y distances between the centroids of the dots was measured in the print pattern of Figure 4-24b and compared with the expected distance of 85 microns between pixels from the pattern below in Figure 4-24a where each dot represents a pixel.

The relative accuracy of the printer is dependent upon several factors, the velocity of the drop as it exits the nozzle, the accuracy of the stage, timing synchronization, and the accuracy of the calibration routine. The accuracy of the Bioprinter is measured using the pattern printed, shown in Figure 4-24. Figure 4-24a gives the dimensions between the

individual dots in pixels, to convert these to actual physical measurements the number of pixels is multiplied by 85 microns. The printed dots are approximately 160~170 microns in diameter. Table 4-1 is a list of the commanded values of the distances between drops and the mean, maximum, and minimum distances measured between drops.

	Pattern Distance	Mean Measured	Maximum Measured	Minimum Measured	Standard Deviation
3 Pixels	258 microns	257.5 microns	269 microns	245 microns	7.61 microns
5 Pixels	430 microns	421 microns	432 microns	416 microns	11.05 microns
6 Pixels	516 microns	501 microns	511 microns	490 microns	8.11 microns
48 Pixels	4128 microns	3972 microns	4029 microns	3931 microns	36.56 microns

Table 4-2 Measurements of Intra-Cartridge Printed Pattern

	Pattern Distance	Mean Measured	Maximum Measured	Minimum Measured	Standard Deviation
1 Pixel	86 microns	84.28 microns	97 microns	74 microns	8.8 microns
3 Pixels	258 microns	227.7 microns	265 microns	204 microns	24.5 microns

Table 4-3 Measurements of Inter-Cartridge Printed Pattern

The data in Table 4-1 shows the distance between same color dots and Table 4-2 shows the distance between the different color dots, there is no error greater than 26 microns between consecutive dots in either direction with no cartridge switch and an error of 156 microns with standard deviation of 36 microns over the whole width of the image e.g. 48 pixels. The error increases in the measurements between different colored dots (the system was calibrated) due to the approximation of dx and dy but the maximum measured error was 54 microns. The repeatability of the horizontal dots was accurate and shown in Figure 4-25, where a line is fit to the motion the stage traversed and the dots center does not vary by more than 20 μm.

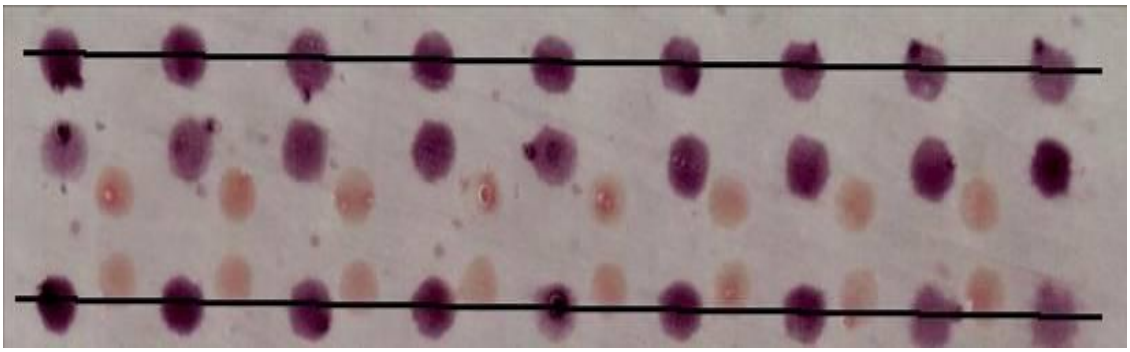

Figure 4-25 Deviation from a Horizontal Line

This accuracy is acceptable considering the error of placement to the size of the drops only being a 1 to 3 ratio and considering the contributing factors to the overall error of x-y placement of drops. The results in the table above provide the verification needed of the accuracy and viability of the Bioprinter as a platform for bioprinting research.

Verification with Cells

With the verification of the system completed with ink, the system was tested using cells and "bio-ink". Alternating lines of two cell types were printed with a vertical distance between each line of 300 microns. The distance between pixels in the x-direction along the lines was kept at the native resolution of the HP26 cartridge of 86 microns. Cells were suspended in a serum-free cell media at a concentration of 7 million cells per milliliter of cell media. Figure 4-26 shows the results of the line patterns, with 4T07 murine mammary epithelial tumor (non-metastatic) cells fluorescing red and D1 murine mesenchymal stem cells fluorescing green.

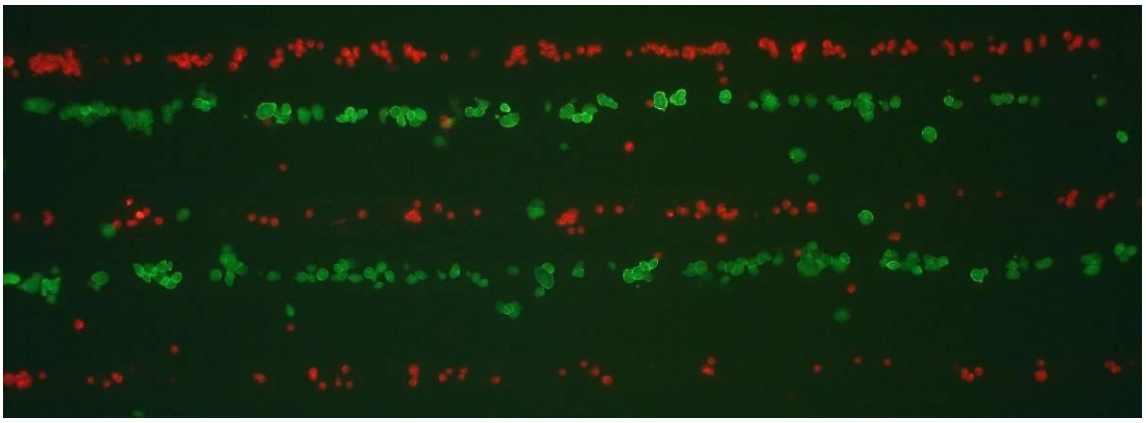

Figure 4-26 Line Pattern Printed With Two Cell Types

The “bio-ink” with cells in suspension printed in similar fashion to the ink versions, with a few satellite drops. These are most likely due to the height of the cartridge when the experiment was run. Figure 4-26 shows the system operating in its intended purpose printing patterns of cells to allow the study of their interactions.

Extension to Three Dimensions

To extend the current 2D Bioprinting system to three dimensions, the most immediate modifications required would be to add another Anaheim Automation stage for the third axis and to modify the Matlab code that controls the system. Additionally, the speed of the system should be increased to make printing multiple layers a viable option, as cells do not remain in suspension for long periods of time. A DC motor used for the x-axis stage would significantly increase the print speed. Using all the nozzles in the printhead during printing would also increase print speed by increasing the amount of surface area covered with one pass of the print media.

CHAPTER FIVE
CONCLUSION

The design of the bioprinting system was developed through a thorough investigation of the printing process in the HP 500 series printer to identify the salient technologies that could be re-used in the bioprinter. The HP26 cartridge with integrated printhead was identified as the one component that contains technology that could not easily be reproduced. A set of specifications were developed to build a 2D printing system that incorporates this cartridge. A design was proposed and a prototype built. The system was shown to print accurately up to 50 microns, even after switching cartridges and printing a second pattern. The capabilities of the system as well as the design considerations for the next revision of the bioprinting system are summarized below.

The bioprinter system presented here is a complete self-contained environment for the design and printing of cell patterns. The bioprinter can print in two full dimensions whereas the modified commercial inkjet printers are limited to the x travel of the printer and the height of the printhead in the y direction. The bioprinter allows for a second cartridge to be installed and calibrated to the first cartridge, thus providing functionality unavailable in the modified inkjet printers. The bioprinter can also be easily adapted to three dimensions with an additional position stage. The system allows for resolution to be set on the fly as well as allowing for adjustment of the amount of energy used to form droplets. These parameters will allow for studies on the effect of varying energy on the vitality of the cells printed. The ability to change resolution allows for studies to be conducted on the effect of single drops of cells printed with varying distance as well as

printing multiple cell types on a small scale. These abilities allow researchers a unique tool to directly address open questions such as the probability of a drop containing a cell and the best concentration of cells for a given cell type.

The main limitation of the designed system is the speed at which it prints a bitmap image. Given real-time systems update clock speed of 1 kHz, the PWM signal used to fire the nozzles of the HP26 cartridge was limited to a 1000 cycles per second; the cartridge can actually be fired at 3.3 kHz. This translates into the ability to only fire a thousand drops a second for a single nozzle. This is not a big problem when patterns are small, but with ever increasing complexities and size of desired patterns, this is an area that needs to be addressed. Another limitation to the speed of the overall system is the motors used to actuate the 2D stage. Stepper Motors were chosen for the initial application due to low cost and the availability of adequate commercial controllers. They however have a speed limitation that could be overcome by switching over to a brushless DC motor as the actuator for the print direction since DC motors are capable of operating at a higher rpm than stepper motors.

Increasing the number of nozzles used to fire from one to all fifty nozzles would significantly increase speed by an order of magnitude. If the height of the printhead was printed with every horizontal pass then the print time would be reduced as the printer would print approximately half a centimeter every pass. Such a significant increase in speed will help reduce the time the cells are exposed out of culture. This improvement could be done with existing hardware and would only require software modifications.

Another limitation that could be resolved in future versions of the Bioprinting system is the implementation of a vision system to provide visual feedback for calibrating multiple printheads, and determination of whether a cell is contained in a drop from the printer. Implementing such a system should be a straightforward with MATLAB's ability to grab frames from a Firewire or USB camera source. The vision system would drastically reduce the amount of time required to run the calibration routine and could provide for more accurate results.

Overall the bioprinter system is a unique tool that will be able to be used to generate important data in the field of tissue engineering such as probability measurements of cells being printed and data regarding the interaction of different cell types printed in precise patterns. There is still work to be done to further this project along; however, there is a sufficient framework in place for this technology to advance at a rapid pace. As the world's population increases the demand for more regenerative and transplantable tissue is sure to increase. This provides the need to further these technologies so that one day the need can be fulfilled with a steady stream of viable, healthy engineered tissue.

REFERENCES

[1] A. Ashkin. The radiation pressure of laser light. Presented at 1972 International Quantum Electronics Conference.

[2] T. Boland, X. Tao, B. J. Damon, B. Manley, P. Kesari, S. Jalota and S. Bhaduri. (2007, Drop-on-demand printing of cells and materials for designer tissue constructs. *Materials Science and Engineering C 27(3),* pp. 372-376. Available: http://dx.doi.org/10.1016/j.msec.2006.05.047

[3] K. J. L. Burg and T. Boland. (2003, Minimally invasive tissue engineering composites and cell printing. *IEEE Engineering in Medicine and Biology Magazine 22(5),* pp. 84-91. Available: http://dx.doi.org/10.1109/MEMB.2003.1256277

[4] T. Burg, R. 1. Groff, K. Burg, M. Hill and T. Boland. Systems engineering challenges in inkjet biofabrication. Presented at IEEE SoutheastCon 2007.

[5] W. A. Buskirk, D. E. Hackleman, S. T. Hall, P. H. Kanarek, R. N. Low, K. E. Trueba and R. R. {. d. Poll}. (1988, oct). Development of a high-resolution thermal inkjet printhead. *Hew\-Lett-Pack\-Ard Journal: Technical Information from the Laboratories of Hew\-Lett-Pack\-Ard Company 39(5),* pp. 55-61.

[6] M. J. DiVittorio, B. Cripe, C. W. Nichols, M. S. Ard, K. R. Hudson and D. J. Neff. (1988, oct). Firmware for a laser-quality thermal inkjet printer. *Hew\-Lett-Pack\-Ard Journal: Technical Information from the Laboratories of Hew\-Lett-Pack\-Ard Company 39(5),* pp. 81-86.

[7] J. P. Harmon and J. A. Widder. (1988, oct). Integrating the printhead into the HP DeskJet printer. *Hew\-Lett-Pack\-Ard Journal: Technical Information from the Laboratories of Hew\-Lett-Pack\-Ard Company 39(5),* pp. 62-66.

[8] R. Langer and J. P. Vacanti. (1993, May 14). Tissue engineering. *Science 260(5110),* pp. 920-926.

[9] D. J. May, M. D. Lund, T. B. Pritchard and C. W. Nichols. (1988, oct). Data to dots in the HP DeskJet printer. *Hew\-Lett-Pack\-Ard Journal: Technical Information from the Laboratories of Hew\-Lett-Pack\-Ard Company 39(5),* pp. 76-80.

[10] V. Mironov, T. Boland, T. Trusk, G. Forgacs and R. R. Markwald. (2003, Apr). Organ printing: Computer-aided jet-based 3D tissue engineering. *Trends Biotechnol. 21(4),* pp. 157-161.

[11] M. Nakamura, A. Kobayashi, F. Takagi, A. Watanabe, Y. Hiruma, K. Ohuchi, Y. Iwasaki, M. Horie, I. Morita and S. Takatani. (2005, Biocompatible inkjet printing technique for designed seeding of individual living cells. *Tissue Eng. 11(11-12),* pp. 1658-1666. Available: http://dx.doi.org/10.1089/ten.2005.11.1658

[12] J. D. Rhodes. (1988, oct). Managing the development of the HP DeskJet printer. *Hew\-Lett-Pack\-Ard Journal: Technical Information from the Laboratories of Hew\-Lett-Pack\-Ard Company 39(5),* pp. 51-54.

[13] R. E. Saunders, J. E. Gough and B. Derby. (2008, Delivery of human fibroblast cells by piezoelectric drop-on-demand inkjet printing. *Biomaterials 29(2),* pp. 193-203. Available: http://dx.doi.org/10.1016/j.biomaterials.2007.09.032

[14] R. Skalak. Tissue engineering. Presented at Proceedings of the 15th Annual International Conference of the IEEE Engineering in Medicine and Biology Society.

[15] D. J. Williams and I. M. 1. Sebastine. (2005, 12/09). Tissue engineering and regenerative medicine: Manufacturing challenges. *IEEE Proceedings-Nanobiotechnology 152(6),* pp. 207-10. Available: http://dx.doi.org/10.1049/ip-nbt:20050001

[16] W. C. Wilson Jr and T. Boland. (2003, Jun). Cell and organ printing 1: Protein and cell printers. *Anat. Rec. A. Discov. Mol. Cell. Evol. Biol. 272(2),* pp. 491-496.

[17] T. Xu, C. A. Gregory, P. Molnar, X. Cui, S. Jalota, S. B. Bhaduri and T. Boland. (2006, Jul). Viability and electrophysiology of neural cell structures generated by the inkjet printing method. *Biomaterials 27(19),* pp. 3580-3588.

[18] T. Xu, J. Jin, C. Gregory, J. J. Hickman and T. Boland. (2005, Jan). Inkjet printing of viable mammalian cells. *Biomaterials 26(1),* pp. 93-99.